Heterogeneous endocrine cell composition defines human islet functional phenotypes

AUTHORS

Carmella Evans-Molina[1,2,3,4,5,6,7,18*], Yasminye D. Pettway[8,18], Diane C. Saunders[9,18], Seth A. Sharp[10,18], Thomas SR. Bate[9], Han Sun[10], Heather Durai[9], Shaojun Mei[9], Anastasia Coldren[9], Corey Davis[9], Conrad V. Reihsmann[9], Alexander L. Hopkirk[9], Jay Taylor[9], Amber Bradley[9], Radhika Aramandla[9], Greg Poffenberger[9], Adel Eskaros[9], Regina Jenkins[9], Danni Shi[11], Hakmook Kang[11], Varsha Rajesh[10], Swaraj Thaman[10], Fan Feng[9], Jean-Philippe Cartailler[12], Alvin C. Powers[8,9,13], Kristin Abraham[14], Anna L. Gloyn[10,15,16*], Joyce C. Niland[17*], and Marcela Brissova[9,19*] on behalf of the Integrated Islet Distribution Program

AUTHOR AFFILIATIONS AND FOOTNOTES

Departments of [1]Pediatrics, [2]Medicine, [3]Anatomy, Cell Biology, and Physiology, and [4]Biochemistry and Molecular Biology, the [5]Center for Diabetes and Metabolic Diseases, and the [6]Herman B. Wells Center for Pediatric Research, Indiana University School of Medicine, Indianapolis, IN 46202, USA

[7]Richard L. Roudebush VA Medical Center, Indianapolis, IN 46202, USA

[8]Department of Molecular Physiology and Biophysics, Vanderbilt University School of Medicine, Nashville, TN 37232, USA

[9]Division of Diabetes, Endocrinology, and Metabolism, Department of Medicine, Vanderbilt University Medical Center, Nashville, TN 37232, USA

[10]Department of Pediatrics, Stanford School of Medicine, Stanford, CA 94305, USA

[11]Department of Biostatistics, Vanderbilt University Medical Center, Nashville, TN 37232, USA

[12]Vanderbilt Center for Stem Cell Biology, Vanderbilt University, Nashville, TN 37232, USA

[13]VA Tennessee Valley Healthcare System, Nashville, TN 37232, USA

[14]Division of Diabetes, Endocrinology, & Metabolic Diseases, National Institutes of Health, Bethesda, MD 20892, USA

[15]Department of Genetics, Stanford School of Medicine, Stanford, CA, USA

[16]Stanford Diabetes Center, Stanford School of Medicine, Stanford, CA, USA

[17]Department of Diabetes and Cancer Discovery Science, Arthur Riggs Diabetes and Metabolism Research Institute, Beckman Research Institute, City of Hope, Duarte, CA 91010, USA

[18]These authors contributed equally

[19]Lead Contact

*Corresponding Authors (in alphabetical order)

Address correspondence and requests for reprints to: Marcela Brissova, marcela.brissova@vanderbilt.edu; Carmella Evans-Molina, cevansmo@iu.edu; Anna L Gloyn, agloyn@stanford.edu; and Joyce C Niland, jniland@coh.org

SUMMARY

Phenotyping and genotyping initiatives within the Integrated Islet Distribution Program (IIDP), the largest source of human islets for research in the U.S., provide standardized assessment of islet preparations distributed to researchers, enabling the integration of multiple data types. Data from islets of the first 299 organ donors without diabetes, analyzed using this pipeline, highlights substantial heterogeneity in islet cell composition associated with hormone secretory traits, sex, reported race and ethnicity, genetically predicted ancestry, and genetic risk for type 2 diabetes (T2D). While α and β cell composition influenced insulin and glucagon secretory traits, the abundance of δ cells showed the strongest association with insulin secretion and was also associated with the genetic risk score (GRS) for T2D. These findings have important implications for understanding mechanisms underlying diabetes heterogeneity and islet dysfunction and may provide insight into strategies for personalized medicine and β cell replacement therapy.

KEYWORDS

Human islets, alpha cells, beta cells, delta cells, insulin secretion, glucagon secretion, T1D, and T2D genetic risk score

INTRODUCTION

Diabetes mellitus impacts over 11% of Americans and is the eighth leading cause of death in the U.S., with an estimated economic cost of over $413 billion annually[1,2]. Type 1 diabetes (T1D) accounts for 5-10% of all diabetes cases and results from autoimmune-mediated destruction and loss of the insulin-producing β cells, whereas type 2 diabetes (T2D), the most prevalent diabetes form, is characterized by β cell dysfunction and peripheral insulin resistance. While the etiologies of T1D and T2D are largely distinct, both forms require loss and/or dysfunction of pancreatic β cells, have a strong genetic component, and are heterogeneous regarding disease pathophysiology, progression, and response to therapeutic interventions [3–7]. Increasingly, data from clinical cohorts, tissues derived from human organ donors and mouse models highlight a role for impaired function of other islet cell subtypes, including α cells and δ abnormalities in diabetes pathophysiology[8–18]. Murine models have advanced our understanding of disease pathophysiology; however, there are critical differences in the function and architecture of murine and human pancreatic islets necessitating the comprehensive study of human islets to translate basic science research findings[19–25].

The Integrated Islet Distribution Program (IIDP), formerly the Islet Cell Resource[26], has served as the main source of human islets for research within the U.S., with nearly 300 million islets supplied for use in more than 600 unique studies to date (https://iidp.coh.org/). Located at City of Hope (Duarte, CA) and funded by the National Institutes of Diabetes and Digestive and Kidney Diseases (NIDDK) with targeted programmatic funding from Breakthrough T1D (formerly JDRF), the IIDP's mission is to distribute high-quality human islets to the diabetes research community to support basic science and translational research. The IIDP subcontracts with a group of expert islet isolation centers at institutions across the country, who procure donated pancreata from their local Organ Procurement Organizations (OPOs). Rigorous protocols are followed to isolate the islets while maximizing the yield, viability and purity. An automated algorithm developed by the IIDP ensures fair and equitable islet distribution, matching the islet offers to awaiting researchers who have subscribed to receive islets and other non-islet biospecimens from the IIDP[27,28].

In response to the NIH's call to enhance rigor, reproducibility, and transparency in biomedical research, the IIDP initiated the Human Islet Phenotyping Program (HIPP) at Vanderbilt University Medical Center and the Human Islet Genotyping Initiative (HIGI) Program at Stanford University to provide systematic phenotypic and genotypic assessment of IIDP-supported human islet preparations (**Extended Data Figure 1**)[29]. This workflow comprehensively evaluates islet morphology, purity, and viability (**Extended Data Figure 2**). For

the first time, it also assesses islet cell composition and concurrently examines the *in vitro* β and α cell function[12,30–35]. It also generates GRS for T1D and T2D while predicting genetic ancestry across a diverse group of organ donors in the U.S. (see **Figure 1A**). This centralized approach reduces redundancy and provides cost savings to investigators to accelerate the speed of scientific discoveries made using these islets. Importantly, the IIDP provides this rich integrated islet data generated by the HIPP and HIGI for researchers to explore via the online IIDP Research Data Repository (RDR). Here, we present an analysis of the first 299 IIDP-supported islet preparations from donors without a clinical diagnosis of diabetes analyzed using the HIPP and HIGI pipelines. Our integrated analysis of this dataset highlights marked heterogeneity in islet secretory traits and points to a previously underappreciated heterogeneity in islet cell composition. We found that the heterogeneity concerning three primary endocrine cell types, α, β, and δ cells, is associated not only with islet hormone secretion traits but also with sex, reported race and ethnicity, genetically predicted ancestry, and T2D GRS. While α and β cell composition influenced insulin and glucagon secretory traits, most notably, the abundance of a relatively small δ cell population showed the strongest association with insulin and glucagon secretion traits. Delta cell composition was also associated with the T2D GRS. These findings have important implications for understanding the mechanisms underlying personalized signatures—whether genetic, functional, or architectural—that predispose individuals to diabetes. Additionally, they may influence the progression and treatment outcomes of the disease, as well as inform β cell replacement therapy using human islets for transplantation.

RESULTS

We present an analysis of the first release of 299 human islet preparations from donors without diabetes, for which all relevant donor information was available (**Figure 1B**). This dataset was derived from a diverse pool of donors with respect to reported race, ethnicity, age, and BMI. Islets from male donors were overrepresented in the dataset (62%), which is reflective of overall trends in available islets and organ donors in the U.S.[36]. The distribution of reported race or ethnicity differed between male and female donors ($p = 0.014$), where the dataset included a higher percentage of female donors that were reported Black or African American (15% vs. 5%, $p = 0.006$). A higher percentage of male donors were Hispanic or Latino, though this difference was not statistically significant). In 90% of the human islet preparations for which genotyping data was available, the genetic ancestry of the donor was predicted ($n = 268$; **Figure 1C**). Overall, there was a high concordance between reported race or ethnicity and primary predicted genetic ancestry within the two datasets ($\kappa = 0.867$, $p < 0.001$). Similar to the

larger dataset, there was a lower percentage of male donors with primary African ancestry (2.5% vs. 16%, p = 0.0002) and a higher proportion of male donors with Admixed American ancestry (38.5% vs. 22%, p = 0.009).

There were no significant differences in age, BMI, or HbA1c between male and female donors by Wilson rank sum test. The mean age of male and female donors was 43 (range 15 – 68 years) and 46 years (range 20 – 65 years), and BMI averaged 29 kg/m^2 in both male (range 13.7 – 46.8 kg/m^2) in female donors (range 17.6 – 47.6 kg/m^2). The mean HbA1c of male and female donors was 5.4% (range 4 – 6.3%) and 5.3% (range 4.3 – 6.4%). Of note, this dataset includes islets from donors within a normal HbA1c range, defined by the American Diabetes Association as <5.7% (n = 223, mean ± SD: 5.2 ± 0.3, range 4.0 – 5.6), as well as a subset of islets from donors with an HbA1c ≥ 5.7% (n = 76, mean ± SD: 5.9 ± 0.2, range 5.7 – 6.4). In the group of donors where genetic ancestry was predicted, the average age was 44 (range 15 – 68 years) and 46 years (range 20 – 65 years) in male and female donors, respectively. The average and distribution of BMI and HbA1c were similar to the larger dataset. Together, these data form a powerful dataset to understand population-based differences in human islet phenotype.

Islet processing traits associated with islet purity and viability

IIDP-affiliated islet isolation centers identify, process donor pancreata, and distribute human islet preparations for phenotypic assessment by the HIPP, genotypic assessment by the HIGI, and scientific investigation by researchers (**Supplemental File 1**). The IIDP RDR includes data on islet purity and viability, which are measured by islet isolation centers and made available to researchers at broadcast (i.e., prior to distribution, at the time the islets are offered to investigators). The post-shipment islet purity and viability is assessed by the HIPP on the day of arrival. The RDR also includes data related to islet processing, including organ cold ischemia duration, pre-shipment culture time, and transit time. The current dataset included human islet preparations from five islet isolation centers: Scharp-Lacy Research Institute (n = 113), Southern California Islet Cell Resource Center (n = 94), University of Miami Diabetes Research Institute (n = 30), University of Pennsylvania Islet Transplant Center (n = 21), and the University of Wisconsin Human Islet Core (n = 35). Pre-shipment culture time averaged 57.5 hours (range 8 – 237 hours), and the average transit time to the HIPP was 25 hours (range 10 – 102 hours). The mean islet purity measured by the HIPP was 73% (range 15 – 95%), and the mean dispersed islet cell viability was 76% (range 43 – 93%). Islet transit time and dispersed cell viability were positively correlated (Spearman r =0.2, unadjusted p-value (p_{unadj}) = 0.001). The

HIPP assessment of islet purity did not show an association with cold ischemia duration, pre-shipment culture time, or islet transit time.

Islet secretory function is highly heterogeneous amongst donors

A dynamic perifusion system was used to investigate simultaneously β and α cell hormone secretion in response to both physiologic and pharmacologic stimuli with co-stimulatory and opposing effects on insulin and glucagon secretion. This included basal glucose (5.6 mM), high glucose (16.7 mM), high glucose with isobutylmethylxanthine (IBMX), low glucose (1.7 mM) with adrenaline (Ad), and potassium chloride (KCl) (**Figure 2A-B**). On average, high glucose led to a 7.9-fold increase in stimulated insulin secretion and inhibited glucagon secretion by 0.4-fold on average compared to basal glucose. In contrast, low glucose with adrenaline led to the opposite effect, reducing insulin secretion by approximately 0.2-fold and increasing glucagon secretion by 5.1-fold compared to basal glucose. Exposure to IBMX, a phosphodiesterase inhibitor that increases intracellular cAMP levels, potentiated glucose-stimulated insulin secretion (14-fold) and stimulated glucagon secretion (6.5-fold) compared to basal glucose level. Additionally, KCl-induced membrane depolarization potently stimulated both insulin and glucagon secretion by approximately 31- and 11-fold on average, respectively.

To understand how biological variables and islet processing features impacted hormone secretion across donors, we derived 11 insulin and 9 glucagon secretion traits from the respective hormone secretion traces (**Figure 2C-D**). For each human islet preparation, we derived the following secretion traits from each insulin trace: basal insulin secretion, glucose-stimulated 1st phase secretion (G 16.7 1st area under the curve; AUC), glucose-stimulated 2nd phase secretion (G 16.7 2nd phase secretion), overall glucose-stimulated insulin secretion (G 16.7 AUC), the glucose stimulation index (SI; G 16.7 SI), cAMP-potentiated insulin secretion (G 16.7 + IBMX 100 AUC), cAMP-potentiated SI (G 16.7 + IBMX 100 SI), response to low glucose plus adrenaline (G 1.7 + Ad 1 AUC), low glucose plus adrenaline inhibition index (II; G 1.7 + Ad 1 II), KCl-mediated insulin secretion (KCl 20 AUC), and KCl stimulation index (KCl 20 SI). We also derived the following secretory traits from each glucagon trace: basal secretion, glucose-inhibited glucagon secretion (G 16.7 AUC), glucose inhibition index (G 16.7 II), cAMP-potentiated glucagon secretion, cAMP-potentiated SI, low glucose plus adrenaline-induced secretion, low glucose plus adrenaline SI, KCl-mediated secretion, and the KCl stimulation index. These data highlight the marked heterogeneity in responses, with the distribution of values shown for the total dataset and separately by sex and reported race and ethnicity or primary predicted ancestry in **Extended Data Tables 1-4**. Spearman correlation analyses revealed a significant correlation between donor age, sex, HbA1c, and BMI with multiple

secretory traits (**Extended Data Figure 3**). Basal insulin secretion was positively correlated with HbA1c ($r = 0.14$, $p_{unadj} = 0.02$) and BMI ($r = 0.14$, $p_{unadj} = 0.02$). Age was negatively correlated with cAMP-potentiated insulin secretion ($r = -0.15$, $p_{unadj} = 0.01$) and the glucose stimulation index ($r = -0.12$, $p_{unadj} = 0.047$). The glucose stimulation index also was negatively correlated with sex ($r = -0.12$, $p_{unadj} = 0.04$), BMI ($r = -0.14$, $p_{unadj} =0.02$), and HbA1c ($r = -0.14$, $p_{unadj} = 0.02$). Additionally, HbA1c was positively correlated with cAMP-potentiated ($r = 0.16$, $p_{unadj} = 0.005$) and KCl-mediated glucagon secretion ($r = 0.12$, $p_{unadj} = 0.04$).

In multivariable models adjusting for donor age, sex, BMI, HbA1c, reported race or ethnicity, and islet isolation center, both pre-shipment culture time and islet transit time were significantly associated with multiple insulin and glucagon secretion traits (**Extended Data Figure 4A-B**). Given this, we added pre-shipment culture time and islet transit time into future multivariable regression models as additional covariates unless otherwise stated (8 covariates total). Of note, islet purity was associated with 3 islet functional traits; however, these data were unavailable for all observations for inclusion as a covariate in the regression model.

To remove potential confounding effects of other demographic and processing variables, we next explored associations between donor traits and secretory traits in multivariable analyses controlling for the other seven covariates. In these analyses, donor BMI was significantly associated with glucagon secretory traits (**Extended Data Figure 4C-F**). Specifically, BMI was negatively associated with basal (regression coefficient, $b = -0.20$, $p = 0.005$) and KCl-mediated depolarization of glucagon secretion ($b = -0.17$, $p = 0.03$) and positively associated with glucose-mediated glucagon inhibition ($b = 0.15$, $p = 0.03$; **Extended Data Figure 4D**). Donor age, sex, and reported race or ethnicity were associated with multiple secretory traits prior to, but not after adjusting for multiple comparisons (**Figure 3-4, Extended Data Figure 4**). Interestingly, we found no differences in insulin or glucagon secretion between donors with HbA1c < 5.7% ($n = 223$) and those with HbA1c ≥ 5.7% ($n = 76$) (**Extended Data Figure 4C-D**).

For the human islet preparations for which genotyping data were available, we explored relationships between predicted genetic ancestry and islet function. We found that the relationships between primary predicted genetic ancestry and secretion were similar to those observed between reported race or ethnicity and insulin secretion. In addition, genetic ancestry had a statistically significant effect on basal insulin secretion (**Extended Data Figure 4E, Extended Data Figure 5A**).

Islet composition strongly influences hormone secretory response

Next, we explored associations between islet function, morphology (i.e., diameter, area, perimeter), composition, and hormone content (**Figure 5**). Interestingly, in both Spearman correlation and multivariable analyses, islet composition was highly associated with multiple secretion traits, especially insulin secretion (**Figure 5A-B, Extended Data Figure 3**). A higher percentage of β cells was associated with an increase in glucose-stimulated ($b = 0.23$, $p = 2.31 \times 10^{-4}$), cAMP-potentiated ($b = 0.35$, $p = 1.18 \times 10^{-8}$), and depolarization-mediated insulin secretion ($b = 0.30$, $p = 1.16 \times 10^{-6}$). These secretory traits were negatively associated with the percentage of islet α and δ cells. Additionally, the percentage of δ cells within the islets was negatively associated with the glucose stimulation index ($b = -0.13$, $p = 0.02$) and inhibition index of insulin secretion in response to low glucose and adrenaline ($b = -0.19$, $p = 1.76 \times 10^{-3}$). These associations were marked by relatively large effect sizes, as evidenced by the absolute value of the scaled regression coefficient (0.13 – 0.35).

Regarding the glucagon secretion traits, the percentage of α cells was positively associated with an increase in basal glucagon secretion ($b = 0.18$, $p = 3.42 \times 10^{-3}$) and total glucagon secreted in response to low glucose with adrenaline ($b = 0.21$, $p = 3.42 \times 10^{-3}$), while the percentage of β cells was negatively associated with these two traits (**Figure 5B**). Additionally, the percentage of α cells was negatively associated with the glucagon stimulation indices in response to both low glucose with adrenaline ($b = -0.17$, $p = 1.58 \times 10^{-2}$) and KCl ($b = -0.18$, $p = 9.28 \times 10^{-3}$), while the opposite was true for their association with the percentage of δ cells.

As expected, β and α cell composition were strongly associated with insulin and glucagon content, respectively (**Figure 5C, Extended Data Figure 3**). However, associations between hormone content were more striking for glucagon secretion traits than insulin secretion traits after controlling for the eight covariates and adjusting for multiple comparisons (**Figure 5A-B**). Glucagon content was strongly associated with multiple glucagon secretion traits (**Figure 5B**), including basal glucagon secretion ($b = 0.40$, $p = 1.13 \times 10^{-13}$) and total glucagon secreted in response to all four secretagogues; further, these associations were marked by relatively large effect sizes (0.21 – 0.42).

In contrast to the impact of islet composition and hormone content, we found no association between morphological traits (diameter, area, perimeter) of islets purified by hand-picking that underwent dynamic perifusion and any insulin or glucagon secretion traits (**Figure 5A-B**). Similar results were found when examining the relationship between the morphology-related traits of the islet preparation as a whole and islet functional traits (**Figure 5A-B**).

Islet composition is influenced by sex, reported race/ethnicity, and predicted genetic ancestry

Given the strong association between islet composition and hormone secretion, we analyzed relationships between islet composition and donor characteristics. On average, analyzed islets were composed of 58% β cells (range 25 – 92%), 34% α cells (range 3 – 68%), and 8% δ cells (range 1 – 19%). Similar to islet hormone secretion, there was significant donor-to-donor heterogeneity in islet endocrine cell composition (**Figure 6A**). Donor sex and reported race or ethnicity had a global effect on the percentage of islet β and α cells in multivariable models incorporating the other seven covariates (**Figure 6B-C**). Specifically, female sex was associated with a higher percentage of α cells and a lower percentage of β cells. Additionally, individuals reported as Asian had a higher percentage of β cells ($p = 0.011$) and a lower percentage of α cells ($p = 0.009$). Similar to relationships observed with reported race, donors with predicted East Asian ancestry had a higher percentage of β cells ($p = 0.007$) and a lower percentage of α cells ($p = 0.005$) versus those with African, Admixed American, or European ancestry (**Figure 6D**). We observed no significant effect of donor age, BMI, HbA1c, isolation center, pre-shipment culture time or islet transit time on islet composition in multivariable analyses (**Extended Data Figure 6A-B**).

We next investigated associations between islet hormone content, donor demographic, and islet processing traits (**Figure 6E-L, Extended Data Figure 6C-D**). Insulin content was positively associated with donor age ($b = 0.14$, $p = 0.0496$) and negatively associated with transit time ($b = -0.15$, $p = 0.03$) in multivariable models controlling for the other seven covariates (**Extended Data Figure 6C-D**). In contrast, we found no associations between insulin content and donor sex, reported race or ethnicity, genetic predicted ancestry, BMI, HbA1c, or isolation center in similar multivariable analyses (**Figure 6F-H; Extended Data Figure 6C-D**). Finally, there was a global effect of sex on glucagon content ($p = 0.015$), but no other associations were noted between glucagon content and other demographic or processing traits in multivariable models (**Figure 5J-L; Extended Data Figure 6C-D**).

Genetic risk for diabetes is associated with islet composition

Both T1D and T2D GWAS signals map to loci associated with islet-enriched genes and their regulatory elements[6,37]. Furthermore, diabetes risk alleles have been associated with *in vivo* measures of islet function in participants without diabetes and linked to worsened islet function in those with T1D[38–40]. Thus, we were interested in determining how genetic risk for diabetes influenced *in vitro* hormone secretion, content, and islet composition in our study. In the current release of human islet preparations where donor genotyping data were available (n

= 268), we generated T1D and T2D GRS, utilizing 67 and 338 single nucleotide variants, respectively, based on previously published models[7,41]. Using these data, we investigated whether genetic risk for diabetes predicted any observed differences in islet function, composition or hormone content in our dataset of human islet preparations from donors without diabetes. We further investigated the role of "process-specific" partitioned genetic risk scores previously published from clustering of intermediate traits to delineate heterogeneity in polygenic risk[42]. We incorporated either the complete or partitioned GRS into multivariable models that included the following as covariates: donor age, BMI, HbA1c, sex, isolation center, pre-shipment culture time, islet transit time, and the first five principal components explaining genetic ancestry (12 covariates total). Interestingly, the T2D GRS was positively associated with the percentage of islet δ cells ($b = 0.17$, $p = 0.019$; **Figure 7**) and, at the same time, δ cells strongly influenced the islet hormone secretory traits (**Figure 5**), especially those of β cells. We detected no significant associations between T1D and T2D GRS and either hormone secretion or content (**Figure 7**). To determine whether donor HbA1c might mediate associations between the calculated GRS and islet secretory traits, hormone content, or composition, we performed a similar analysis excluding HbA1c as a covariate (**Extended Data Figure 7**). The significant association between the T2D GRS and the percentage of islet δ cells remained; however, we also detected a significant positive association between the T2D GRS and glucagon content (**Extended Data Figure 7**).

DISCUSSION

Islet physiology is disrupted in both T1D and T2D. The pathways and cell-cell communications that underlie islet dysfunction in diabetes are poorly understood, yet they may have important implications in treatment strategies employing both pharmacologic agents and islet or β cell replacement therapy. Recent emphasis on precision medicine approaches coupled with increased utilization of single-cell technologies has highlighted an important role for heterogeneity in diabetes classification, treatment, and molecular phenotypes[43–47]. To understand how biological variation in humans impacts islet function and diabetes risk, we generated this research resource from islets distributed through the NIH-funded IIDP. These islets underwent pre-shipment assessment at one of five islet isolation centers followed by centralized phenotyping and genotyping through the HIPP and HIGI programs. A strength of our study is the inclusion of islets from a diverse group of U.S. organ donors with over 40% of donors having a reported race or ethnicity other than White, non-Hispanic or Latino/a. The IIDP-HIPP-HIGI workflow has enabled investigation for associations between inherent donor

267 characteristics, islet composition, genetic risk scores for T1D and T2D, and multiple insulin and
268 glucagon secretory traits. Our data can be accessed through the IIDP RDR, where researchers
269 can view and interrogate the dataset used for this analysis and propose their own unique
270 questions related to human islet biology using the larger RDR dataset. Images presented in this
271 report are available on the open access Pancreatlas™ platform[48], which supports interactive
272 exploration of full-resolution islet imaging data.

273 Our phenotyping workflow includes an assessment of islet purity and viability, insulin and
274 glucagon secretion measured in a dynamic perifusion system, and a quantitative assessment of
275 islet composition in a sample of islets distinct from the islet aliquot used for perifusion. Studies
276 of the human pancreas suggest a greater than four-fold variation in β cell mass amongst
277 individuals without diabetes[49]. Not surprisingly, we observed a wide range of β cell secretory
278 responses to glucose, IBMX, and KCl, in line with previous reports [50–52]. While clinical studies
279 suggest that glucose tolerance declines with age, whether β cell function declines with age
280 independently of changes in insulin resistance and weight in individuals who maintain normal
281 glucose tolerance is not clear[53,54]. Similarly, the impact of donor age on insulin secretion *in vitro*
282 has been mixed in previous reports, with studies finding either no effect or a negative impact of
283 age on glucose-stimulated insulin secretion[51,55–58]. In addition, many studies report an effect of
284 BMI on multiple insulin secretory traits, while others have found no correlation[50,51,57,59]. In the
285 current study, Spearman correlation analyses revealed a significant positive relationship
286 between BMI and basal insulin secretion and a negative relationship between either BMI or age
287 and the glucose stimulation index. However, we detected no significant association between any
288 donor trait and insulin secretion in multivariable regression models adjusting for 7 other donor
289 and islet processing-related covariates. Our studies differ from these previous studies in that we
290 included a larger sample size of donors and controlled for multiple potentially confounding
291 demographic and islet processing features, which we and others have shown to impact *in vitro*
292 secretory responses[51,57,60].

293 In contrast to the weak effects of donor demographics on insulin secretion, islet
294 composition exhibited strong and consistent associations with insulin secretory traits in both
295 Spearman correlation and multivariable analyses. Consistent with observed heterogeneity in
296 hormone secretory responses, islet composition was highly heterogeneous amongst islet
297 preparations, with an approximately 4, 22, and 19-fold variation in the percentages of β, α, and
298 δ cells, respectively. Beta cell composition or a higher percentage of β cells was associated with
299 increased glucose-stimulated, cAMP-potentiated, and depolarization-mediated insulin secretion.
300 While islet isolation severs vascular and neuronal connections, the autonomy of the islet as a

301 mini-organ is well preserved after isolation, as demonstrated by the persistence of paracrine
302 interactions and electrical coupling that modulate islet cell-cell communication within islets[61].
303 Interestingly, although δ cells comprised a relatively low percentage of islet endocrine cell
304 composition, a higher percentage of δ cells negatively impacted most insulin secretion traits.
305 This finding is notable given a recent report showing that δ cells regulate the glycemic set point
306 in healthy mice and that ablation of the δ cell population leads to blood glucose lowering and
307 increased insulin secretion[62].

308 Finally, compared to studies that have assessed islet insulin secretion, considerably less
309 is known about the impact of donor and processing traits on *in vitro* glucagon secretion in islets
310 from organ donors without diabetes[63]. In living individuals without diabetes, Fræch and
311 colleagues reported an inverse relationship between fasting glucagon levels and insulin
312 sensitivity in individuals with normal glucose tolerance[11]. Individuals with reduced insulin
313 sensitivity also displayed impaired glucagon suppression in response to an oral glucose
314 challenge, even after adjusting for plasma glucose levels[11]. We found that higher BMI was
315 associated with lower basal glucagon levels and depolarization-induced glucagon secretion *in*
316 *vitro*; however, consistent with the previous study, total glucagon secreted in response to high
317 glucose was higher, suggesting impaired glucose-mediated glucagon suppression.

318 The mechanisms that regulate glucagon secretion are not well understood but likely
319 include a combination of intrinsic and paracrine mechanisms[64,65]. Multiple glucagon secretory
320 traits were associated with islet composition; however, we found even stronger associations
321 between glucagon content and total glucagon secreted in response to all secretagogues used in
322 this study. Interestingly, this same relationship was not observed between insulin content and
323 insulin secretory responses. One study comparing murine β and α cells noted faster rates of
324 glucagon granule exocytosis, larger readily releasable pools, and a higher rate of refilling of
325 these pools after depletion in α cells[66]. Therefore, it is possible that these same mechanisms are
326 at play in human islets and could explain differences in the association between hormone
327 content and secretion between β and α cells.

328 Our observations on the impact of islet composition on secretory traits raise an important
329 question of whether differences in cell composition are influenced by donor demographics
330 and/or genetics. Interestingly, we found a global effect of sex and reported race or ethnicity on
331 the percentage of islet β and α cells. Here, female donors had a higher percentage of α cells,
332 and donors reported as Asian exhibited a higher percentage of β cells. We note the relatively
333 small number of donors reported as Asian in the dataset, highlighting a need to confirm this
334 observation with larger sample sizes. Remarkably, a high T2D GRS was positively associated

with the percentage of islet δ cells, which was consistent with the finding that δ cell composition negatively impacted most insulin secretion traits, highlighting the inhibitory potential of δ cell-secreted factors, including somatostatin. Together, these data suggest that, in some individuals, a genetic predisposition to having more δ cells may impact insulin secretory capacity and glycemic setpoints, making one more susceptible to the development of T2D. However, the mechanisms by which genetic variation associated with altered T2D risk influences δ cell composition are unknown. Recent studies have utilized the abundance of known endocrine marker proteins to infer associations with gene and protein expression[52,60]; however, this is the first time to our knowledge that direct quantitative assessment of islet composition has been compared to hormone secretion.

In summary, this study has identified important relationships between donor demographics, genetics, islet processing, islet composition, hormone content, function, using human islet preparations from donors without diabetes. Given their impact on human islet function, these factors should be considered in interpreting future human islet studies. Further, they may have implications in strategies for β cell replacement therapy[67]. For example, in 2022 the FDA approved Lantidra[68], the first allogeneic pancreatic islet cellular therapy made from deceased donor pancreatic cells for the treatment of T1D to ameliorate problematic hypoglycemia with glucocorticoid-free immunosuppression[69]. Release criteria for islet grafts have historically included measures of glucose-stimulated insulin secretion. Our data highlight the impact of cell-cell interactions on islet function and suggest that islet composition may provide valuable insight into graft function post-transplant. Similarly, we expect that integrating these findings from 299 donors without diabetes with datasets generated using the same phenotyping and genotyping pipelines for islets from individuals with T1D and T2D, such as those generated by the Human Pancreas Analysis Program (HPAP)[70,71] will inform our understanding of diabetes pathophysiology and lead to the design of new therapies and disease prevention. Further, whilst we examined factors impacting glucose-stimulated islet responses in detail, we did not investigate responses to other nutrients, such as fatty acids or amino acids, which also display significant donor-to-donor heterogeneity, as highlighted by a recent report from Kolic et al[52]. Finally, while this study is currently the largest of its type, we had multiple observations that were nominally significant, supporting the need for larger studies and expanded sample sizes. The diverse IIDP-HIPP-HIGI datasets represent a valuable and continuously growing resource for the islet biology community that may be used to generate new scientific hypotheses and guide mechanistic studies of human islets.

RESOURCE AVAILABILITY

Lead Contact

Further information and requests for resources and reagents should be directed to and will be fulfilled by the lead contact, Marcela Brissova, PhD (marcela.brissova@vumc.org). Requests for access to genetic data should be directed to Anna L Gloyn, DPhil (agloyn@stanford.edu).

Materials Availability

This study did not generate new unique reagents.

Data and code availability

Data from the first release of 299 de-identified human islet preparations reported in this paper is available in **Supplemental File 2.** The genetic risk scores and predicted ancestry for each donor and the larger integrated dataset hosted are available for download from the IIDP Research Data Repository. For more information on available datasets and how to access visit https://iidp.coh.org/Resources-Offered/Research-Data-Repository. Genotyping data has been deposited in the European Genome Phenome Archive (EGA) and will be available at publication through a data access agreement.

All original code is publicly available as of the date of publication. Code related to generation of statistical models is available at https://github.com/hakmook/HIPP_project. Code related to prediction of genetic ancestry is available at https://github.com/gloynlab/GeneticAncestry.

Any additional information required to reanalyze the data reported in this paper is available from the lead contact upon request.

ACKNOWLEDGMENTS

The authors would like to thank the organ donors and their families for their invaluable donations and acknowledge the IIDP collaborators who continue to make this work possible (**Supplemental File 1**). The authors would also like to thank Danielle Gibson (Vanderbilt University Medical Center) for her assistance to the HIPP and Dr. Emily Anderson-Baucum (Indiana University School of Medicine) for her helpful advice and edits. Research reported in this publication was supported by U42 RR017673, UC4 DK098085, U24 DK098085, 1-RSC-2018-561-I-X, 1-RSC-2019-712-S-B, 1-RSC-2020-890-S-B, F30DK134041, T32GM007347,

T32GM152284, and The Leona M. and Harry B. Helmsley Charitable Trust. Whole-slide imaging was performed in the Islet and Pancreas Analysis Core of the Vanderbilt DRTC (DK20593).

AUTHOR CONTRIBUTIONS

Conceptualization: M.B., Y.D.P., H.K., D.C.S., S.A.S., A.L.G., J.C.N., and C.E.M.; Data curation: Y.D.P., D.C.S., S.A.S., H.S., A.L.K., A.B., and F.F.; Formal analysis: H.K., D.S., Y.D.P., S.A.S., and D.C.S.; Funding acquisition: C.E.M., K.A., A.L.G., J.C.N., and M.B.; Investigation: H.D., S.M., A.C., C.D., C.V.R., J.T., T.SR.B., R.A., G.P., A.E., R.J. V.S., and S.T.; Methodology: S.A.S., H.S., D.S., H.K., A.C.P., S.A.S. H.S. A.L.G and M.B.; Project administration: C.E.M., K.A., A.L.G., J.C.N., and M.B.; Software: JP.C.; Resources: M.B., C.E.M., A.L.G., J.C.N., JP.C., and A.C.P.; Supervision: M.B., C.E.M., A.L.G, J.C.N., H.K., A.C.P., and K.A.; Visualization: Y.D.P. and D.C.S.; Writing – original draft: Y.D.P., C.E.M., and M.B.; Writing – review & editing: all authors

DECLARATION OF INTERESTS

A.L.G's spouse is an employee of Genentech and holds stock options in Roche.

411 **FIGURE LEGENDS**

412 **Figure 1. Integration of phenotyping and genotyping assessment of a diverse set of IIDP-**
413 **derived human islet preparations.** (**A**) Schematic illustrating the human islet phenotyping and
414 genotyping pipelines utilized by the HIPP and HIGI. The HIPP performs analysis of islet
415 morphology, purity, viability, histology, and function; the remaining sample is archived in a
416 biorepository for additional analyses. The HIGI receives a non-islet tissue sample and isolates
417 DNA to sequence for genetic ancestry prediction and calculation of genetic risk scores for type 1
418 and type 2 diabetes. (**B**) Descriptive statistics of donor demographics by sex and reported race
419 or ethnicity (n = 299). Values are reported as mean ± standard deviation, followed by the range.
420 (**C**) Descriptive statistics of donor demographics by sex and primary predicted ancestry (n =
421 268). Values are reported as mean ± standard deviation, followed by the range. **p < 0.01 vs.
422 male donors; ***p < 0.001 vs. male donors.

423 **Figure 2. Islet secretory function is highly heterogeneous amongst donors.** Average (**A**)
424 insulin and (**B**) glucagon secretion from donor islets normalized to islet equivalents (IEQs). Data
425 are displayed as mean ± 95% confidence interval (n = 299). (C) Schematic and tables
426 describing insulin and (**D**) glucagon secretion traits derived from individual islet secretion traces.
427 Descriptive statistics by sex and reported race/ethnicity are provided in **Extended Data Tables**
428 **1 and 2**. G – Glucose (mM); IBMX – isobutylmethylxanthine (μM); A – adrenaline (μM); KCl –
429 potassium chloride (mM).

430 **Figure 3. Islet secretion traits by sex.** Violin plots comparing (**A**) insulin and (**B**) glucagon
431 secretion traits between female (n = 115) and male (n = 184) donors. The solid line in each
432 violin plot depicts the median, and the dotted lines represent the 1st and 3rd quartiles. Global P-
433 value is based on the F-test while controlling for the seven covariates (age, sex, BMI, HbA1c,
434 islet isolation center, pre-shipment culture time, and islet transit time) and adjusting for multiple
435 comparisons. Comparisons where the unadjusted p-value (p_{unadj}) was significant are noted in
436 italics.

437 **Figure 4. Islet secretion traits by reported race or ethnicity.** Violin plots comparing (**A**)
438 insulin and (**B**) glucagon secretion traits by reported race or ethnicity (n = 12 Asian, n = 26 Black
439 or African American, n = 86 Hispanic or Latino/a, n = 175 White). The solid line in each violin
440 plot depicts the median, and the dotted lines represent the 1st and 3rd quartiles. Global p-value is
441 based on the F-test while controlling for the seven covariates (age, sex, BMI, HbA1c, islet
442 isolation center, pre-shipment culture time, and islet transit time) and adjusting for multiple

443 comparisons. Comparisons where the unadjusted p-value (p_{unadj}) was significant are noted in
444 italics.

445 **Figure 5. Islet composition and hormone content are associated with multiple islet**
446 **secretory traits.** (**A-B**) Heatmaps depicting regression coefficients of each morphologic
447 variable for islets that underwent perifusion (n = 186), islet composition variable (n = 299), and
448 total islet insulin and glucagon content (n = 299) after being incorporated into multivariable
449 regression models controlling for age, sex, BMI, HbA1c, islet isolation center, reported race or
450 ethnicity, pre-shipment culture time, and islet transit time for each (**A**) insulin or (**B**) glucagon
451 secretion trait. (**C**) Heatmaps depicting regression coefficients of each islet composition variable
452 after being incorporated into multivariable regression models for total insulin or glucagon
453 content after adjusting for the eight covariates (n = 299). Adjusted p-values are indicated where
454 *p < 0.05, **p < 0.01, and ***p < 0.001. Comparisons where the unadjusted p-value (p_{unadj}) was
455 significant are noted in italics.

456 **Figure 6. Islet composition and hormone content are highly variable and influenced by**
457 **donor sex and ancestry.** (**A**) Representative images of collagen gel-embedded islets and
458 associated quantification of islet composition (n = 299). Violin plots comparing islet composition
459 by (**B**) donor sex, (**C**) reported race or ethnicity, and (**D**) predicted primary genetic ancestry. (**E**)
460 Islet insulin content normalized to IEQ (n = 299). Violin plots comparing islet insulin content by
461 (**F**) donor sex, (**G**) reported race or ethnicity, and (**H**) predicted primary genetic ancestry. (**F**) Islet
462 glucagon content normalized to IEQ (n = 299). Violin plots comparing islet glucagon content by
463 (**J**) donor sex, (**K**) reported race or ethnicity, and (**L**) predicted primary genetic ancestry. Donor
464 sex: n = 115 female, n = 184 male. Reported race or ethnicity: n = 12 Asian, n = 26 Black or
465 African American, n = 86 Hispanic or Latino/a, n = 175 White. Primary predicted genetic
466 ancestry: n = 86 Admixed American, n = 21 African, n = 11 East Asian, n = 150 European. *p <
467 0.05, **p < 0.01. For sex, reported race or ethnicity, and genetic ancestry, the global adjusted p-
468 value is based on the F-test while controlling for the other seven covariates. INS – insulin; GCG
469 – glucagon; SST – somatostatin.

470 **Figure 7. Associations between genetic risk scores for type 1 and type 2 diabetes and**
471 **islet function, hormone content, and composition.** (**A-B**) Heatmaps depicting coefficients of
472 the GRS for (**A**) T1D and (**B**) T2D along with partitioned GRS variables after being incorporated
473 into multivariable regression models for each secretion trait, hormone content, and islet
474 composition variable (n = 268). Each model included the following covariates: donor age, sex,
475 BMI, HbA1c, islet isolation center, pre-shipment culture time, islet transit time, and the first 5

476 principal components explaining primary genetic ancestry. “T1D GRS” encompasses the genetic
477 risk for T1D (67 total variants). “HLA DR/DQ” represents the sum of T1D risk at HLA-DR/DQ
478 haplotypes. “HLA Class 1” and “HLA Class 2” represent the sum of T1D risk at HLA class 1 and
479 2 alleles, respectively, excluding HLA DR/DQ haplotypes. “Non-HLA” represents the sum of T1D
480 risk from variants outside the HLA region, genome-wide. “T2D GRS” encompasses genetic risk
481 for T2D (338 total variants). “Beta Cell,” “Proinsulin,” “Obesity,” “Lipodystrophy,” and “Liver/Lipid”
482 represent partitioned T2D GRS clusters encoding the related variants. *$p < 0.05$. Comparisons
483 where the unadjusted p-value (p_{unadj}) was significant are noted in italics.

EXTENDED DATA FIGURE AND TABLE LEGENDS

Extended Data Figure 1, related to Figure 1. Schematic of multimodal data integration by phenotyping and genotyping pipelines within Integrated Islet Distribution Program (IIDP) and data deposition in Resource Data Repository (RDR).

Extended Data Figure 2, related to Figure 1. Example HIPP procedures. (**A**) Representative images of a human islet preparation stained with dithizone (DTZ) to delineate islet versus non-islet tissue. Using the Count and Measure function in cellSens, images of DTZ-stained islets were utilized to quantify the total islet equivalents (IEQs), purity, and islet morphology. Tissue depicted in red on the image mark-up indicates positively identified islet tissue, while green marks non-islet tissue. (**B**) Representative images of handpicked islets pre- and post-perifusion. The red color on the image markup indicated positively identified islet tissue by the Count and Measure function in cellSens. The scale bar is 500 μm.

Extended Data Table 1, related to Figure 2. Insulin secretion is highly heterogeneous amongst donors. Descriptive statistics of the eleven insulin secretion traits by donor sex and reported race or ethnicity. Data are displayed as mean ± SD, followed by the range.

Extended Data Table 2, related to Figure 2. Glucagon secretion is highly heterogeneous amongst donors. Descriptive statistics of the nine glucagon secretion traits by donor sex and reported race or ethnicity. Data are displayed as mean ± SD, followed by the range.

Extended Data Table 3, related to Figure 2. Distribution of insulin secretion traits is similar in n = 268 subset. Descriptive statistics of the eleven insulin secretion traits by donor sex and genetic ancestry. Data are displayed as mean ± SD, followed by the range.

Extended Data Table 4, related to Figure 2. Distribution of glucagon secretion traits is similar in n = 268 subset. Descriptive statistics of the nine glucagon secretion traits by donor sex and genetic ancestry. Data are displayed as mean ± SD, followed by the range.

Extended Data Figure 3, related to Figure 2. Relationship between donor demographics, islet processing, islet morphology, and functional traits. Heatmap of Spearman r correlation coefficients between the indicated variables in the corresponding labeled row and column. For donor sex, the male was coded as 0 and female as 1. *$p < 0.05$; †$p < 0.01$; ‡$p < 0.001$. All p-values are unadjusted.

Extended Data Figure 4, related to Figures 3 and 4. Donor and islet processing traits correlate with islet function. (**A-B**) Heatmaps depicting regression coefficients of each islet

515 processing trait after being incorporated into multivariable regression models for each (**A**) insulin
516 and (**B**) glucagon secretion trait. Each model included the following covariates: age, sex,
517 reported race or ethnicity, BMI, HbA1c, and islet isolation center. Pre-shipment culture time and
518 islet transit time were included as additional covariates for all subsequent models, unless noted
519 otherwise. (**C-D**) Heatmaps depicting regression coefficients of donor age, BMI, and
520 prediabetes status after being incorporated into multivariable regression models for each (**C**)
521 insulin and (**D**) glucagon secretion trait while controlling for the other seven final covariates.
522 Adjusted p-values are indicated where *p < 0.05, **p < 0.01, and **p < 0.001. For associations
523 that are significant prior to adjusting to multiple comparisons, the unadjusted p-value is noted in
524 italics. (**E-F**) Tables summarizing the global P-value when comparing differences by donor sex,
525 reported race or ethnicity, genetic ancestry, and isolation center for each (**E**) insulin and (**F**)
526 glucagon secretion trait. The global p-value is based on the F-test while controlling for the other
527 seven covariates. Analyses involving genetic ancestry controlled for all covariates except
528 reported race or ethnicity. n.s. indicates an insignificant global adjusted p-value and un-adjusted
529 p-values. For results that were significant prior to adjusting to multiple comparisons, the
530 unadjusted p-value is noted in italics. n = 299 for all analyses except those involving islet purity
531 (n = 269), elevated HbA1c (n = 76 elevated HbA1c, n = 223 normal HbA1c), and genetic
532 ancestry (n = 268).

533 **Extended Data Figure 5, related to Figure 4. Islet secretion traits by genetic ancestry.**
534 Violin plots comparing (**A**) insulin and (**B**) glucagon secretion traits by primary predicted genetic
535 ancestry (n = 86 Admixed American, n = 21 African, n = 11 East Asian, n =150 European). The
536 solid line in each violin plot depicts the median, and the dotted lines represent the 1st and 3rd
537 quartiles. *p < 0.05 after adjusting for multiple comparisons. Comparisons where the unadjusted
538 p-value (p_{unadj}) was significant are noted in italics. Global p-value is based on the F-test while
539 controlling for the seven covariates (donor age, sex, BMI, HbA1c, islet isolation center, pre-
540 shipment culture time, and islet transit time).

541 **Extended Data Figure 6, related to Figure 6. Correlation between donor demographic and**
542 **islet processing variables with islet composition and hormone content.** (**A**) Heatmaps
543 depicting regression coefficients of donor and islet processing variables when incorporated into
544 multivariable regression models with a composition variable (% β, α, or δ cells) as the outcome
545 variable. For models related to islet processing traits, the following covariates were included:
546 donor age, sex, reported race or ethnicity, BMI, HbA1C, and islet isolation center. For donor
547 traits, pre-shipment culture time and islet transit time were also included as covariates. (**B**) Table

548 summarizing the global p-value when comparing differences by isolation center for each
549 composition variable. The global p-value is based on the F-test while controlling for the other
550 seven covariates. (**C**) Heatmaps depicting regression coefficients of donor and islet processing
551 variables when incorporating into multivariable regression models insulin and glucagon content.
552 For models related to islet processing traits, the following covariates were included: age, sex,
553 reported race or ethnicity, BMI, HbA1C, and islet isolation center. For donor traits, pre-shipment
554 culture time and islet transit time were also included as covariates. (**D**) Table summarizing the
555 global P-value when comparing differences by isolation center for hormone content. The global
556 P-value is based on the F-test while controlling for the other seven covariates. (**E**) Correlation
557 between insulin content with donor age, and (**F**) transit time. n = 299 for all analyses; n.s.
558 indicates insignificant global adjusted p-value and unadjusted p-values.

559 **Extended Data Figure 7, related to Figure 7. Associations between T1D/T2D GRSs and**
560 **islet function, hormone content, and composition, disregarding HbA1c.** (**A-B**) Heatmaps
561 depicting coefficients of the GRS for (**A**) T1D and (**B**) T2D along with partitioned GRS variables
562 after being incorporated into multivariable regression models for each secretion, hormone
563 content, and islet composition variable (n = 268). Each model included the following covariates:
564 donor age, sex, BMI, islet isolation center, pre-shipment culture time, islet transit time, and the
565 first five principal components explaining primary genetic ancestry. *p < 0.05. For associations
566 that are significant prior to adjusting to multiple comparisons, the unadjusted p-value is noted in
567 italics.

568 **METHODS**
569
570 **EXPERIMENTAL MODEL AND STUDY PARTICIPANT DETAILS**
571
572 *Primary human islet isolation*
573 Human islet preparations from cadaveric organ donors (n = 299) were isolated from five
574 affiliated islet isolation centers across the U.S and distributed to the Human Islet Phenotyping
575 Program through the IIDP from 2016-2024. Donor demographic information is detailed in **Figure**
576 **1**. De-identified human pancreatic specimens do not qualify as human subjects research under
577 the Vanderbilt or the Stanford Institutional Review Boards. All assays were performed on the
578 day of islet arrival. Islet preparations included in this manuscript (n = 299) were isolated from
579 five IIDP-affiliated isolation centers: Scharp-Lacy (n = 113), Southern California Islet Cell
580 Resource Center (n = 94), University of Miami (n = 30), University of Pennsylvania Islet
581 Transplant Center (n = 27), and the University of Wisconsin Human Islet Core (n = 35).

582 **METHOD DETAILS**

583 All human islet preparations were assessed according to standardized protocols
584 established by the HIPP and HIGI of the IIDP and are publicly available at
585 https://iidp.coh.org/SOPs. All HIPP-related assessments are conducted on the day-of-arrival.
586 Methods are briefly summarized below:

587 *Islet Purity and Morphology*

588 A representative sample of the unpicked human islet preparation was prepared by
589 combining a 320 µL aliquot of islet preparation and 680 µL CMRL medium. The representative
590 sample was stained with 50 µL of 1 mg/mL dithizone/DMSO/PBS (DTZ; Sigma, catalog #D5130)
591 for 1-2 min at room temperature. After adding 1 mL of CMRL medium, brightfield and darkfield
592 images of stained islets were captured at 10X magnification. Islet (stained) and non-islet
593 (unstained) area was determined using the Count and Measure function in cellSens (Olympus).
594 Islet purity was calculated as the following:

595 $$Islet\ Purity\ (\%) = \frac{Total\ islet\ tissue\ area}{Total\ islet\ tissue\ area + Total\ non-islet\ tissue\ area} \times 100$$

596 Using the Count and Measure function in cellSens, morphological characteristics of each
597 islet were also determined, including average islet radius, diameter, perimeter, and area.
598 Measurements were performed in triplicate to ensure accuracy.

599 *Islet Viability*

600 Qualitative assessment of islet viability upon arrival to the HIPP was performed using
601 fluorescein diacetate (FDA) and propidium iodide (PI). In brief, 400 µL of well-mixed total islet
602 suspension was added to a cell culture dish, and 10 µL of PI (Sigma Aldrich, catalog # P4170)
603 and 10 µL of FDA (Sigma Aldrich, catalog # F-7378) were added to the islet suspension in
604 succession. The plate was incubated in the dark for 15 mins, and the preparation was imaged
605 immediately using an Olympus SZX12 stereomicroscope system. Multiple fields of view were
606 captured from two replicates per donor to ensure that FDA/PI staining was visualized in 50-100
607 islets per preparation.

608 Additionally, a quantitative assessment of islet viability upon arrival to the HIPP was
609 performed using trypan blue dye. Two aliquots of ~100 handpicked islets were prepared in 1.5
610 mL tubes and washed three times using 2 mM EDTA/PBS via centrifugation at 200 rcf for 1 min
611 at 4 °C. Islets were dispersed into a single cell suspension using Accutase (Innovative Cell
612 Technologies, Inc, catalog # AT-104) and triturated at a slow speed for 10 minutes using an
613 electronic multichannel pipet with tips. The reaction was quenched with CMRL-1066 media

614 containing 10% FBS, 2 mM L-glutamine, and 1% penicillin/streptomycin, and cells were washed
615 twice via centrifugation at 500 rcf for 3 mins at 4 °C. The cell pellet was resuspended in 50-75
616 µL of CMRL-1066 medium by gently flicking the tube. Next, 10 µL of the cell suspension was
617 transferred to a new 1.5 mL tube and mixed with 10 µL Trypan Blue dye (Invitrogen, catalog #
618 T10282). The cell chamber slide was loaded with 10 µL of the mixture in each compartment,
619 and cell counts were acquired using the Countess II cell counter following instrument guidelines.
620 Cell counts were repeated for the second aliquot of handpicked islets. Reported viability
621 represents the average percentage of viable cells for duplicates of purified islets based on two
622 cell counts per aliquot.

623 *Islet Function in a Dynamic Perifusion System*

624 Islet function was assessed via dynamic perifusion. On the day islets were received, half
625 of the islet shipment (1000-5000 islet equivalents (IEQs)) was plated in a 10-cm non-tissue
626 culture treated dish and cultured in CMRL-1066 plus 10% FBS media at 37 °C and 5% CO_2 for
627 2 hours prior to perifusion. Under microscope guidance, 267-300 IEQs were handpicked, islet
628 size and count were recorded, and high-resolution brightfield and darkfield images were
629 captured at 10x magnification. All islets were then transferred to a clear Eppendorf tube for
630 loading into the perifusion chamber, fractions were collected at 1 mL/min, and secretagogues
631 were changed at predetermined fractions. The following secretagogues were used for these
632 perifusion studies: 5.6 mM glucose (baseline media; G 5.6), 16.7 mM glucose (G 16.7), 16.7
633 mM glucose with 100 µM isobutylmethylxanthine (IBMX; G 16.7 + IBMX 100), 1.7 mM glucose
634 with 1 µM adrenaline (G 1.7 + Ad 1), and 5.6 mM glucose with 20 mM KCl (G 5.6 + KCl 20). All
635 secretagogues were prepared in a perifusion medium containing 3.2 g $NaHCO_3$, 0.58 g L-
636 glutamine, 0.11 g sodium pyruvate, 1.11 g HEPES, 1 bottle DMEM, 1 g RIA-grade BSA, and 70
637 mg ascorbate in 1 L ultra-purified water. The perifusion medium was filtered and de-gassed prior
638 to preparation of secretagogues.

639 After retrieving islets from the perifusion chamber and placing them into a 60-mm non-
640 treated culture dish, the IEQ of the retrieved islets was determined and islets were centrifuged
641 for 3 min at 200 rcf at room temperature. Islet hormone extracts were prepared by incubating
642 the retrieved islet pellet in 200 µL of fresh acid ethanol (50 µL 5N HCl + 5.5 mL 95% ethanol) for
643 24 hours. Samples were then spun at 3000 rcf for 5 min, aliquoted to 2 mL screwcap tubes, and
644 stored at -80 °C until further processing.

645 Insulin concentration in perifusates and islet extracts was measured via ELISA (2020 –
646 present; Human Insulin ELISA Kit, Mercodia, catalog # 10-1113-10) or RIA (Human Insulin-
647 Specific RIA, Millipore catalog # HI-14K). In the same samples, glucagon was also measured

648 via ELISA or RIA (2021 – present: Quantikine Glucagon ELISA Kit, R&D Systems catalog #
649 DGCG0; 2020 – 2021: HTRF Glucagon Detection Kit, Cisbio catalog #62CGLPEH; prior to
650 2020: Glucagon RIA, Millipore catalog #GL-32K). For each assay, standards and quality
651 controls were measured in duplicates, and perifusate and islet extract samples were measured
652 in duplicates (RIA) or single point (ELISA). Secreted insulin and glucagon concentrations were
653 normalized to IEQs and expressed as ng/100 IEQs/min. Alternatively, secreted insulin and
654 glucagon concentrations were normalized to their respective total hormone content and
655 expressed as %content/min.

656 *Islet Composition*

657 To assess islet composition and acinar cell components, an aliquot of the human islet
658 preparation was immobilized in a collagen I gel, embedded, and sectioned for histologic
659 analysis. An aliquot containing approximately 500 IEQs of the human islet preparation was
660 transferred into a 1.5 mL tube and washed three times in 1X PBS via centrifugation at 200 *xg* for
661 3 min. After removing the supernatant, 150 µL of collagen I working solution (563 µL collagen I
662 stock, 167 µL ultrapurified H_2O, 200 µL 5X DMEM, 20 µL HEPES, and 50 µL $NaHCO_3$) was
663 added to the islet pellet and the mixture was transferred into a well in the center of a 96-well
664 plate. The plate was incubated at 37 °C for 1.5 hours to allow the gel to solidify, then fixed on ice
665 for 15 min, filling the well with cold 4% paraformaldehyde/PBS. After the brief fixation, the
666 paraformaldehyde solution was removed and, using a 28 G needle, the gel was loosened from
667 the sides of the well and transferred with a spatula into a 12-well plate containing cold 4%
668 paraformaldehyde/PBS. The gel was fixed for an additional 45 min, shaking on ice, before being
669 washed three times with 1X PBS for 20 min shaking on ice, transferring the gel to a new well
670 containing fresh 1X PBS for each wash. Following an overnight incubation in 30% sucrose/1X
671 PBS, the collagen I gel was embedded into cryomolds containing OCT, imaged, and flash frozen
672 on dry ice. Islet gels were stored at -80 °C until sectioning.

673 Following sectioning of collagen gels, immunofluorescence staining of islets was
674 performed. In brief, 8-µm islet cryosections were allowed to thaw at room temperature and air-
675 dried for 30 mins. Sections were washed with 1X PBS 3 times for 5 mins to remove the OCT,
676 permeabilized with 0.2% Triton for 15 mins at room temperature, and washed 3 times in 1X
677 PBS. Sections were blocked with 5% normal donkey serum in 1X PBS at room temperature for
678 90 mins in a humidified chamber, then incubated overnight at 4 °C in a humidified chamber with
679 primary antibodies diluted in 0.1% Triton-X-100/1% BSA/1X PBS. Primary antibodies included:
680 C-peptide (rat, Developmental Studies Hybridoma Bank, GN-ID4, RRID:AB_2631151, 1:100),
681 Glucagon (mouse, Abcam, ab10988, RRID:AB_297642, 1:250), Glucagon (rabbit, Cell Signaling

682 Technology, 2760S, RRID:AB_659831, 1:100), Somatostatin (goat, Santa Cruz Biotechnology,
683 sc-7819, RRID:AB_2302603, 1:500), and HPX1 (mouse, Novus Biologicals, NBP1-18951,
684 RRID:AB_1625456, 1:100). Sections were washed with 1X PBS 3 times for 10 mins each, then
685 incubated for 1.5 hours at room temperature in a humidified chamber with secondary antibodies
686 diluted in 0.1% Triton/1% BSA/1X PBS. Secondary antibodies were purchased from Jackson
687 ImmunoResearch: Rat IgG-Cy2 (donkey, 712-225-150, RRID:AB_2340673, 1:500), Rat IgG-
688 Cy5 (donkey, 712-175-150, RRID:AB_2340671, 1:200), Mouse IgG-Cy3 (donkey, 715-165-150,
689 RRID:AB_2340813, 1:500), Rabbit IgG-Cy5 (donkey, 711-175-152, RRID:AB_2340607, 1:200),
690 Goat IgG-Cy5 (donkey, 705-175-147, RRID:AB_2340415, 1:200), and Mouse IgG-Cy3 (donkey,
691 715-165-150, RRID:AB_2340813, 1:500). Sections were counterstained with 1:25,000
692 DAPI/PBS for 10 mins at room temperature, then washed 3 times for 15 mins each in 1X PBS.
693 Sections were mounted with SlowFade Gold mounting medium, and islet sections were imaged
694 using a high-resolution whole slide scanning system (ScanScope FL, Aperio/Leica) connected
695 to a web-based digital slide repository powered by eSlide Manager and housed in the Vanderbilt
696 University Medical Center Data Center. A quantitative assessment of islet cell composition and
697 endocrine/acinar cell compartments was performed using a tissue classifier algorithm (Halo™,
698 Indica Labs) to analyze 50-100 islets per labeling experiment. Images presented herein are
699 deposited in the publicly available Pancreatlas™ platform[48], which allows the exploration of full-
700 resolution islet imaging data in an interactive manner
701 (https://pancreatlas.org/datasets/853/explore).

702 *Genetic Analysis*

703 DNA on 246/299 donors included in this release was isolated from human islet donor
704 acinar tissue at Vanderbilt using the Wizard Genomic DNA Purification Kit (Promega, catalog #
705 A1120). Quantification and quality assessment was performed using the Genomic DNA
706 ScreenTape assay. DNA was normalized to 50 ng/µL prior to shipment to the HIGI for further
707 analysis. For 30 samples no acinar tissue was available. For 9 of these, DNA was extracted
708 from FPPE sections at Stanford using the Zymo QuickDNA FFPE Extraction Kit. For the
709 remaining 23 donors DNA was isolated from acinar tissue at Stanford using the DNAExtraction
710 (Qiagen DNeasyBlood&TissueKit, catalog # 69504).

711 Prior to genotyping all DNA samples were re-quantified using both the Nanodrop and
712 Qubit platforms. Samples containing less than 500 ng total DNA were speed-vacuumed and
713 concentrated prior to genotyping. All samples were genotyped using the Illumina Infinium
714 Omni2.5Exome V1.5 array with ~2.6 million single nucleotide variant (SNV) sites measured.
715 Genotyping data underwent quality control by filtering of SNVs with excess missing genotypes

716 (>2%), filtering of SNVs that do not conform to Hardy-Weinberg equilibrium (p<1x10^-6), and
717 removal of samples with either excess missing genotypes (>3%) or discordant genetic vs
718 recorded sex. For donor samples with excess missing genotypes, 10 um thick formalin-fixed
719 paraffin embedded pancreas tissue slides were requested from IIDP. DNA was extracted using
720 the Zymo QuickDNA FFPE Extraction Kit and quantified by Nanodrop and Qubit. Samples were
721 then restored using the Infinium HD FFPE Restore Protocol and then re-genotyped. Since FFPE
722 samples have considerable DNA degradation, if these samples did not pass restoration, thicker
723 20 um FFPE slides were shipped from IIDP and DNA was extracted and sent for restoration and
724 genotyping. For samples that had discordant sex, an XY PCR was performed on the original
725 sample and an additional donor sample from IIDP (10-μm thick formalin-fixed paraffin-
726 embedded pancreas tissue slides). From the 270 donors passing QC coordinates were then
727 aligned to the positive strand on genome build GRCh38 and the data imputed against the
728 TOPMed R3 reference panel. After quality control and imputation, 69.4 million high-quality SNVs
729 (R2 > 0.3) and 269 samples were available for analysis. Genetic risk scores (GRS) for T1D and
730 T2D were generated from previously published models using 67 and 338 SNVs respectively[7,41].
731 T2D partitioned genetic risk scores (pGRS) were generated using 94 SNVs with predetermined
732 weights from a previous soft-clustering[42]. Genetic ancestry was determined using a random
733 forest classifier trained on the first 20 principal components of the 1000 Genomes reference
734 panel (https://github.com/gloynlab/GeneticAncestry).

735 **QUANTIFICATION AND STATISTICAL ANALYSIS**

736 *Hormone secretion traits*

737 Using the insulin and glucagon secretion traces normalized to IEQ, eleven insulin
738 secretion traits and nine glucagon secretion traits were defined and calculated as illustrated in
739 **Figure 2C-D**.

740 *Statistical analysis*

741 To determine demographic, islet processing, and morphologic variables associated with
742 differences in islet secretory function, we first performed Spearman correlation analyses. For
743 variables with a statistically significant association with islet secretory traits, we utilized
744 multivariable regression models to examine the relationship among the explanatory variables
745 and the outcome variable of interest. For each model, we controlled for the following potential
746 confounders, unless otherwise noted: donor age, sex, BMI, isolation center, HbA1c, reported
747 race or ethnicity, pre-shipment culture time, and transit time. A statistically significant regression

coefficient for the explanatory variable (p-value < 0.05) denoted a significant association. Given multiple p-values, we adjusted for the false discovery rate (FDR) at 0.05 to control for multiple comparisons.

Similarly, to explore potential differences based on prediabetes status or sex, we used multivariable regression models. In these models, an indicator variable (0 for normal, 1 for pre-diabetes participants; 0 for male, 1 for female) acted as the explanatory variable. For prediabetes-related associations, we controlled for all eight of the aforementioned potential confounders except HbA1c. For sex-related associations, we controlled all potential confounders except donor sex. The significance of the regression coefficient (b) for the group indicator (p-value < 0.05) indicated a notable difference in the outcome variable between the two groups.

To ensure comparability of regression coefficients across models, we normalized the outcome variables and all continuous explanatory variables, including covariates. This normalization involved centering the variables by subtracting their mean and scaling them by their standard deviation. However, this procedure was not applied to categorical covariates in the model, such as center, self-reported ancestry, and sex. Statistical analyses were all performed using R Statistical Software version 4.3.0 (R Foundation for Statistical Computing, Vienna, Austria) and GraphPad Prism version 10.

REFERENCES

1. Centers for Disease Control and Prevention National Diabetes Statistics Report. https://www.cdc.gov/diabetes/php/data-research/index.html.

2. Parker, E.D., Lin, J., Mahoney, T., Ume, N., Yang, G., Gabbay, R.A., ElSayed, N.A., and Bannuru, R.R. (2023). Economic Costs of Diabetes in the U.S. in 2022. Diabetes Care *47*, 26–43. https://doi.org/10.2337/dci23-0085.

3. Mattis, K.K., and Gloyn, A.L. (2020). From Genetic Association to Molecular Mechanisms for Islet-cell Dysfunction in Type 2 Diabetes. J. Mol. Biol. *432*, 1551–1578. https://doi.org/10.1016/j.jmb.2019.12.045.

4. Viñuela, A., Varshney, A., Bunt, M. van de, Prasad, R.B., Asplund, O., Bennett, A., Boehnke, M., Brown, A.A., Erdos, M.R., Fadista, J., et al. (2020). Genetic variant effects on gene expression in human pancreatic islets and their implications for T2D. Nat Commun *11*, 4912. https://doi.org/10.1038/s41467-020-18581-8.

5. Rich, S.S., Erlich, H., and Concannon, P. (2018). Genetics of Type 1 Diabetes. In Diabetes in America. 3rd edition. Bethesda (MD): National Institute of Diabetes and Digestive and Kidney Diseases (US), C. C. Cowie, S. S. Casagrande, A. Menke, M. A. Cissell, M. S. Eberhardt, J. B. Meigs, E. W. Gregg, W. C. Knowler, E. Barrett-Connor, D. J. Becker, et al., eds., p. Chapter 12.

6. Krentz, N.A.J., and Gloyn, A.L. (2020). Insights into pancreatic islet cell dysfunction from type 2 diabetes mellitus genetics. Nat. Rev. Endocrinol. *16*, 202–212. https://doi.org/10.1038/s41574-020-0325-0.

7. Mahajan, A., Spracklen, C.N., Zhang, W., Ng, M.C.Y., Petty, L.E., Kitajima, H., Yu, G.Z., Rüeger, S., Speidel, L., Kim, Y.J., et al. (2022). Multi-ancestry genetic study of type 2 diabetes highlights the power of diverse populations for discovery and translation. Nat. Genet. *54*, 560–572. https://doi.org/10.1038/s41588-022-01058-3.

8. Unger, R.H., Aguilar-Parada, E., Müller, W.A., and Eisentraut, A.M. (1970). Studies of pancreatic alpha cell function in normal and diabetic subjects. J Clin Invest *49*, 837–848. https://doi.org/10.1172/jci106297.

9. Gerich, J.E., Langlois, M., Noacco, C., Karam, J.H., and Forsham, P.H. (1973). Lack of Glucagon Response to Hypoglycemia in Diabetes: Evidence for an Intrinsic Pancreatic Alpha Cell Defect. Science *182*, 171–173. https://doi.org/10.1126/science.182.4108.171.

10. Sherr, J., Tsalikian, E., Fox, L., Buckingham, B., Weinzimer, S., Tamborlane, W.V., White, N.H., Arbelaez, A.M., Kollman, C., Ruedy, K.J., et al. (2014). Evolution of Abnormal Plasma Glucagon Responses to Mixed-Meal Feedings in Youth With Type 1 Diabetes During the First 2 Years After Diagnosis. Diabetes Care *37*, 1741–1744. https://doi.org/10.2337/dc13-2612.

11. Færch, K., Vistisen, D., Pacini, G., Torekov, S.S., Johansen, N.B., Witte, D.R., Jonsson, A., Pedersen, O., Hansen, T., Lauritzen, T., et al. (2016). Insulin Resistance Is Accompanied by Increased Fasting Glucagon and Delayed Glucagon Suppression in Individuals With Normal and Impaired Glucose Regulation. Diabetes *65*, 3473–3481. https://doi.org/10.2337/db16-0240.

12. Brissova, M., Haliyur, R., Saunders, D., Shrestha, S., Dai, C., Blodgett, D.M., Bottino, R., Campbell-Thompson, M., Aramandla, R., Poffenberger, G., et al. (2018). α Cell Function and Gene Expression Are Compromised in Type 1 Diabetes. Cell Reports *22*, 2667–2676. https://doi.org/10.1016/j.celrep.2018.02.032.

13. Camunas-Soler, J., Dai, X.-Q., Hang, Y., Bautista, A., Lyon, J., Suzuki, K., Kim, S.K., Quake, S.R., and MacDonald, P.E. (2020). Patch-Seq Links Single-Cell Transcriptomes to Human Islet Dysfunction in Diabetes. Cell Metab *31*, 1017-1031.e4. https://doi.org/10.1016/j.cmet.2020.04.005.

14. Omar-Hmeadi, M., Lund, P.-E., Gandasi, N.R., Tengholm, A., and Barg, S. (2020). Paracrine control of α-cell glucagon exocytosis is compromised in human type-2 diabetes. Nat Commun *11*, 1896. https://doi.org/10.1038/s41467-020-15717-8.

15. Kellard, J.A., Rorsman, N.J.G., Hill, T.G., Armour, S.L., Bunt, M. van de, Rorsman, P., Knudsen, J.G., and Briant, L.J.B. (2020). Reduced somatostatin signalling leads to hypersecretion of glucagon in mice fed a high-fat diet. Mol. Metab. *40*, 101021. https://doi.org/10.1016/j.molmet.2020.101021.

16. Vergari, E., Denwood, G., Salehi, A., Zhang, Q., Adam, J., Alrifaiy, A., Asterholm, I.W., Benrick, A., Chibalina, M.V., Eliasson, L., et al. (2020). Somatostatin secretion by Na+-dependent Ca2+-induced Ca2+ release in pancreatic delta cells. Nat. Metab. *2*, 32–40. https://doi.org/10.1038/s42255-019-0158-0.

17. Dai, X.-Q., Camunas-Soler, J., Briant, L.J.B., Santos, T. dos, Spigelman, A.F., Walker, E.M., Drigo, R.A. e, Bautista, A., Jones, R.C., Avrahami, D., et al. (2021). Heterogenous impairment of α cell function in type 2 diabetes is linked to cell maturation state. Cell Metab *34*, 256-268.e5. https://doi.org/10.1016/j.cmet.2021.12.021.

18. Hill, T.G., Gao, R., Benrick, A., Kothegala, L., Rorsman, N., Santos, C., Acreman, S., Briant, L.J., Dou, H., Gandasi, N.R., et al. (2024). Loss of electrical β-cell to δ-cell coupling underlies impaired hypoglycaemia-induced glucagon secretion in type-1 diabetes. Nat. Metab., 1–12. https://doi.org/10.1038/s42255-024-01139-z.

19. Brissova, M., Fowler, M.J., Nicholson, W.E., Chu, A., Hirshberg, B., Harlan, D.M., and Powers, A.C. (2005). Assessment of Human Pancreatic Islet Architecture and Composition by Laser Scanning Confocal Microscopy. J Histochem Cytochem *53*, 1087–1097. https://doi.org/10.1369/jhc.5c6684.2005.

20. Cabrera, O., Berman, D.M., Kenyon, N.S., Ricordi, C., Berggren, P.-O., and Caicedo, A. (2006). The unique cytoarchitecture of human pancreatic islets has implications for islet cell function. Proc National Acad Sci *103*, 2334–2339. https://doi.org/10.1073/pnas.0510790103.

21. Rodriguez-Diaz, R., Abdulreda, M.H., Formoso, A.L., Gans, I., Ricordi, C., Berggren, P.-O., and Caicedo, A. (2011). Innervation Patterns of Autonomic Axons in the Human Endocrine Pancreas. Cell Metab. *14*, 45–54. https://doi.org/10.1016/j.cmet.2011.05.008.

22. Dai, C., Brissova, M., Hang, Y., Thompson, C., Poffenberger, G., Shostak, A., Chen, Z., Stein, R., and Powers, A.C. (2012). Islet-enriched gene expression and glucose-induced insulin secretion in human and mouse islets. Diabetologia *55*, 707–718. https://doi.org/10.1007/s00125-011-2369-0.

23. Brissova, M., Shostak, A., Fligner, C.L., Revetta, F.L., Washington, M.K., Powers, A.C., and Hull, R.L. (2015). Human Islets Have Fewer Blood Vessels than Mouse Islets and the Density of Islet Vascular Structures Is Increased in Type 2 Diabetes. J. Histochem. Cytochem. *63*, 637–645. https://doi.org/10.1369/0022155415573324.

24. Alcazar, O., and Buchwald, P. (2019). Concentration-Dependency and Time Profile of Insulin Secretion: Dynamic Perifusion Studies With Human and Murine Islets. Front. Endocrinol. *10*, 680. https://doi.org/10.3389/fendo.2019.00680.

25. Gloyn, A.L., Ibberson, M., Marchetti, P., Powers, A.C., Rorsman, P., Sander, M., and Solimena, M. (2022). Every islet matters: improving the impact of human islet research. Nat. Metab. *4*, 970–977. https://doi.org/10.1038/s42255-022-00607-8.

26. Kaddis, J.S., Olack, B.J., Sowinski, J., Cravens, J., Contreras, J.L., and Niland, J.C. (2009). Human Pancreatic Islets and Diabetes Research. Jama *301*, 1580–1587. https://doi.org/10.1001/jama.2009.482.

27. Qian, D., Kaddis, J., and Niland, J.C. (2007). A matching algorithm for the distribution of human pancreatic islets. Comput. Stat. Data Anal. *51*, 5494–5506. https://doi.org/10.1016/j.csda.2007.02.030.

28. Niland, J.C., Stiller, T., Cravens, J., Sowinski, J., Kaddis, J., and Qian, D. (2010). Effectiveness of a Web-Based Automated Cell Distribution System. Cell Transplant. *19*, 1133–1142. https://doi.org/10.3727/096368910x505486.

29. Brissova, M., Niland, J.C., Cravens, J., Olack, B., Sowinski, J., and Evans-Molina, C. (2019). The Integrated Islet Distribution Program answers the call for improved human islet phenotyping and reporting of human islet characteristics in research articles. Diabetologia *62*, 1312–1314. https://doi.org/10.1007/s00125-019-4876-3.

30. Haliyur, R., Tong, X., Sanyoura, M., Shrestha, S., Lindner, J., Saunders, D.C., Aramandla, R., Poffenberger, G., Redick, S.D., Bottino, R., et al. (2018). Human islets expressing HNF1A variant have defective β cell transcriptional regulatory networks. J. Clin. Investig. *129*, 246–251. https://doi.org/10.1172/jci121994.

31. Hart, N.J., Aramandla, R., Poffenberger, G., Fayolle, C., Thames, A.H., Bautista, A., Spigelman, A.F., Babon, J.A.B., DeNicola, M.E., Dadi, P.K., et al. (2018). Cystic fibrosis–related diabetes is caused by islet loss and inflammation. JCI Insight *3*, e98240. https://doi.org/10.1172/jci.insight.98240.

32. Shrestha, S., Saunders, D.C., Walker, J.T., Camunas-Soler, J., Dai, X.-Q., Haliyur, R., Aramandla, R., Poffenberger, G., Prasad, N., Bottino, R., et al. (2021). Combinatorial transcription factor profiles predict mature and functional human islet α and β cells. Jci Insight *6*, e151621. https://doi.org/10.1172/jci.insight.151621.

33. Haliyur, R., Walker, J.T., Sanyoura, M., Reihsmann, C.V., Shrestha, S., Aramandla, R., Poffenberger, G., Ramirez, A.H., Redick, S.D., Babon, J.A.B., et al. (2021). Integrated Analysis of the Pancreas and Islets Reveals Unexpected Findings in Human Male With Type 1 Diabetes. J Endocr Soc *5*, bvab162. https://doi.org/10.1210/jendso/bvab162.

34. Doliba, N.M., Rozo, A.V., Roman, J., Qin, W., Traum, D., Gao, L., Liu, J., Manduchi, E., Liu, C., Golson, M.L., et al. (2022). α Cell dysfunction in islets from nondiabetic, glutamic acid decarboxylase autoantibody–positive individuals. J. Clin. Investig. *132*, e156243. https://doi.org/10.1172/jci156243.

35. Walker, J.T., Saunders, D.C., Rai, V., Chen, H.-H., Orchard, P., Dai, C., Pettway, Y.D., Hopkirk, A.L., Reihsmann, C.V., Tao, Y., et al. (2023). Genetic risk converges on regulatory networks mediating early type 2 diabetes. Nature *624*, 621–629. https://doi.org/10.1038/s41586-023-06693-2.

36. Organ Procurement and Transplantation Network (OPTN), and Scientific Registry of Transplant Recipients (SRTR) (2024). OPTN/SRTR 2022 Annual Data Report. U.S. Department of Health and Human Services, Health Resources and Services Administration; 2024.

37. Fløyel, T., Kaur, S., and Pociot, F. (2015). Genes Affecting β-Cell Function in Type 1 Diabetes. Curr. Diabetes Rep. *15*, 97. https://doi.org/10.1007/s11892-015-0655-9.

38. Dimas, A.S., Lagou, V., Barker, A., Knowles, J.W., Mägi, R., Hivert, M.-F., Benazzo, A., Rybin, D., Jackson, A.U., Stringham, H.M., et al. (2014). Impact of Type 2 Diabetes Susceptibility Variants on Quantitative Glycemic Traits Reveals Mechanistic Heterogeneity. Diabetes *63*, 2158–2171. https://doi.org/10.2337/db13-0949.

39. Brorsson, C.A., Nielsen, L.B., Andersen, M.L., Kaur, S., Bergholdt, R., Hansen, L., Mortensen, H.B., Pociot, F., Størling, J., and Diabetes, H.S.G. on C. (2016). Genetic Risk Score Modelling for Disease Progression in New-Onset Type 1 Diabetes Patients: Increased Genetic Load of Islet-Expressed and Cytokine-Regulated Candidate Genes Predicts Poorer Glycemic Control. J. Diabetes Res. *2016*, 9570424. https://doi.org/10.1155/2016/9570424.

40. Snethlage, C.M.F., Balvers, M., Ferwerda, B., Rampanelli, E., Groen, P. de, Roep, B.O., Herrema, H., McDonald, T.J., Raalte, D.H. van, Weedon, M.N., et al. (2024). Associations between diabetes-related genetic risk scores and residual beta cell function in type 1 diabetes: the GUTDM1 study. Diabetologia, 1–12. https://doi.org/10.1007/s00125-024-06204-6.

41. Sharp, S.A., Rich, S.S., Wood, A.R., Jones, S.E., Beaumont, R.N., Harrison, J.W., Schneider, D.A., Locke, J.M., Tyrrell, J., Weedon, M.N., et al. (2019). Development and Standardization of an Improved Type 1 Diabetes Genetic Risk Score for Use in Newborn Screening and Incident Diagnosis. Diabetes Care *42*, 200–207. https://doi.org/10.2337/dc18-1785.

42. DiCorpo, D., LeClair, J., Cole, J.B., Sarnowski, C., Ahmadizar, F., Bielak, L.F., Blokstra, A., Bottinger, E.P., Chaker, L., Chen, Y.-D.I., et al. (2022). Type 2 Diabetes Partitioned Polygenic Scores Associate With Disease Outcomes in 454,193 Individuals Across 13 Cohorts. Diabetes Care *45*, 674–683. https://doi.org/10.2337/dc21-1395.

43. Tobias, D.K., Merino, J., Ahmad, A., Aiken, C., Benham, J.L., Bodhini, D., Clark, A.L., Colclough, K., Corcoy, R., Cromer, S.J., et al. (2023). Second international consensus report on gaps and opportunities for the clinical translation of precision diabetes medicine. Nat. Med. *29*, 2438–2457. https://doi.org/10.1038/s41591-023-02502-5.

44. Dorrell, C., Schug, J., Canaday, P.S., Russ, H.A., Tarlow, B.D., Grompe, M.T., Horton, T., Hebrok, M., Streeter, P.R., Kaestner, K.H., et al. (2016). Human islets contain four distinct subtypes of β cells. Nat. Commun. *7*, 11756. https://doi.org/10.1038/ncomms11756.

45. Wigger, L., Barovic, M., Brunner, A.-D., Marzetta, F., Schöniger, E., Mehl, F., Kipke, N., Friedland, D., Burdet, F., Kessler, C., et al. (2021). Multi-omics profiling of living human pancreatic islet donors reveals heterogeneous beta cell trajectories towards type 2 diabetes. Nat Metabolism *3*, 1017–1031. https://doi.org/10.1038/s42255-021-00420-9.

46. Weng, C., Gu, A., Zhang, S., Lu, L., Ke, L., Gao, P., Liu, X., Wang, Y., Hu, P., Plummer, D., et al. (2023). Single cell multiomic analysis reveals diabetes-associated β-cell heterogeneity driven by HNF1A. Nat. Commun. *14*, 5400. https://doi.org/10.1038/s41467-023-41228-3.

47. Wang, G., Chiou, J., Zeng, C., Miller, M., Matta, I., Han, J.Y., Kadakia, N., Okino, M.-L., Beebe, E., Mallick, M., et al. (2023). Integrating genetics with single-cell multiomic measurements across disease states identifies mechanisms of beta cell dysfunction in type 2 diabetes. Nat. Genet. *55*, 984–994. https://doi.org/10.1038/s41588-023-01397-9.

48. Saunders, D.C., Messmer, J., Kusmartseva, I., Beery, M.L., Yang, M., Atkinson, M.A., Powers, A.C., Cartailler, J.-P., and Brissova, M. (2020). Pancreatlas: Applying an Adaptable Framework to Map the Human Pancreas in Health and Disease. Patterns *1*, 100120. https://doi.org/10.1016/j.patter.2020.100120.

49. Meier, J.J., Butler, A.E., Saisho, Y., Monchamp, T., Galasso, R., Bhushan, A., Rizza, R.A., and Butler, P.C. (2008). β-Cell Replication Is the Primary Mechanism Subserving the Postnatal Expansion of β-Cell Mass in Humans. Diabetes *57*, 1584–1594. https://doi.org/10.2337/db07-1369.

50. Kayton, N.S., Poffenberger, G., Henske, J., Dai, C., Thompson, C., Aram, la, R., Shostak, A., Nicholson, W., Brissova, M., et al. (2015). Human islet preparations distributed for research exhibit a variety of insulin-secretory profiles. Am J Physiol Endocrinol Metab *308*, E592–E602. https://doi.org/10.1152/ajpendo.00437.2014.

51. Henquin, J. (2018). Influence of organ donor attributes and preparation characteristics on the dynamics of insulin secretion in isolated human islets. Physiol. Rep. *6*, e13646. https://doi.org/10.14814/phy2.13646.

52. Kolic, J., Sun, W.G., Cen, H.H., Ewald, J.D., Rogalski, J.C., Sasaki, S., Sun, H., Rajesh, V., Xia, Y.H., Moravcova, R., et al. (2024). Proteomic predictors of individualized nutrient-specific insulin secretion in health and disease. Cell Metab. *36*, 1619-1633.e5. https://doi.org/10.1016/j.cmet.2024.06.001.

53. Chang, A.M., Smith, M.J., Galecki, A.T., Bloem, C.J., and Halter, J.B. (2006). Impaired β-Cell Function in Human Aging: Response to Nicotinic Acid-Induced Insulin Resistance. J. Clin. Endocrinol. Metab. *91*, 3303–3309. https://doi.org/10.1210/jc.2006-0913.

54. Ferrannini, E., Natali, A., Muscelli, E., Nilsson, P.M., Golay, A., Laakso, M., Beck-Nielsen, H., Mari, A., and Investigators, R. (2011). Natural history and physiological determinants of changes in glucose tolerance in a non-diabetic population: the RISC Study. Diabetologia *54*, 1507–1516. https://doi.org/10.1007/s00125-011-2112-x.

55. Ihm, S.-H., Matsumoto, I., Sawada, T., Nakano, M., Zhang, H.J., Ansite, J.D., Sutherland, D.E.R., and Hering, B.J. (2006). Effect of Donor Age on Function of Isolated Human Islets. Diabetes *55*, 1361–1368. https://doi.org/10.2337/db05-1333.

56. Niclauss, N., Bosco, D., Morel, P., Demuylder-Mischler, S., Brault, C., Milliat-Guittard, L., Colin, C., Parnaud, G., Muller, Y.D., Giovannoni, L., et al. (2011). Influence of Donor Age on Islet Isolation and Transplantation Outcome. Transplantation *91*, 360–366. https://doi.org/10.1097/tp.0b013e31820385e6.

57. Lyon, J., Fox, J.E.M., Spigelman, A.F., Kim, R., Smith, N., O'Gorman, D., Kin, T., Shapiro, A.M.J., Rajotte, R.V., and MacDonald, P.E. (2016). Research-Focused Isolation of Human Islets From Donors With and Without Diabetes at the Alberta Diabetes Institute IsletCore. Endocrinology *157*, 560–569. https://doi.org/10.1210/en.2015-1562.

58. Shrestha, S., Erikson, G., Lyon, J., Spigelman, A.F., Bautista, A., Fox, J.E.M., Santos, C. dos, Shokhirev, M., Cartailler, J.-P., Hetzer, M.W., et al. (2022). Aging compromises human islet beta cell function and identity by decreasing transcription factor activity and inducing ER stress. Sci Adv *8*, eabo3932. https://doi.org/10.1126/sciadv.abo3932.

59. D'Aleo, V., Guerra, S.D., Gualtierotti, G., Filipponi, F., Boggi, U., Simone, P.D., Vistoli, F., Prato, S.D., Marchetti, P., and Lupi, R. (2010). Functional and Survival Analysis of Isolated

Human Islets. Transplant. Proc. *42*, 2250–2251. https://doi.org/10.1016/j.transproceed.2010.05.132.

60. Ewald, J.D., Lu, Y., Ellis, C.E., Worton, J., Kolic, J., Sasaki, S., Zhang, D., Santos, T. dos, Spigelman, A.F., Bautista, A., et al. (2024). HumanIslets.com: Improving accessibility, integration, and usability of human research islet data. Cell Metab. https://doi.org/10.1016/j.cmet.2024.09.001.

61. Walker, J.T., Saunders, D.C., Brissova, M., and Powers, A.C. (2021). The Human Islet: Mini-organ with Mega-impact. Endocr Rev *42*, bnab010-. https://doi.org/10.1210/endrev/bnab010.

62. Huang, J.L., Pourhosseinzadeh, M.S., Lee, S., Krämer, N., Guillen, J.V., Cinque, N.H., Aniceto, P., Momen, A.T., Koike, S., and Huising, M.O. (2024). Paracrine signalling by pancreatic δ cells determines the glycaemic set point in mice. Nat. Metab. *6*, 61–77. https://doi.org/10.1038/s42255-023-00944-2.

63. Pettway, Y.D., Saunders, D.C., and Brissova, M. (2023). The human α cell in health and disease. J Endocrinol. https://doi.org/10.1530/joe-22-0298.

64. Walker, J.N., Ramracheya, R., Zhang, Q., Johnson, P.R.V., Braun, M., and Rorsman, P. (2011). Regulation of glucagon secretion by glucose: paracrine, intrinsic or both? Diabetes, Obes. Metab. *13*, 95–105. https://doi.org/10.1111/j.1463-1326.2011.01450.x.

65. Hughes, J.W., Ustione, A., Lavagnino, Z., and Piston, D.W. (2018). Regulation of islet glucagon secretion: Beyond calcium. Diabetes Obes Metabolism *20*, 127–136. https://doi.org/10.1111/dom.13381.

66. Barg, S. (2003). Mechanisms of Exocytosis in Insulin-Secreting B-Cells and Glucagon-Secreting A-Cells. Pharmacol. Toxicol. *92*, 3–13. https://doi.org/10.1034/j.1600-0773.2003.920102.x.

67. Perez-Frances, M., Bru-Tari, E., Cohrs, C., Abate, M.V., Gurp, L. van, Furuyama, K., Speier, S., Thorel, F., and Herrera, P.L. (2024). Regulated and adaptive in vivo insulin secretion from islets only containing β-cells. Nat. Metab. *6*, 1791–1806. https://doi.org/10.1038/s42255-024-01114-8.

68. RIOS, P., MCGARRIGLE, J.J., LAMONICA, G., LI, Y., COOK, J., JOSHI, I., GHANI, S., COOK, D., LOPEZ, D., NASIR, H., et al. (2024). 35-OR: Lantidra, First FDA-Approved Cellular Therapy to Treat Type 1 Diabetes. Diabetes *73*. https://doi.org/10.2337/db24-35-or.

69. Shapiro, A.M., Lakey, J.R., Ryan, E.A., Korbutt, G.S., Toth, E., Warnock, G.L., Kneteman, N.M., and Rajotte, R.V. (2000). Islet transplantation in seven patients with type 1 diabetes mellitus using a glucocorticoid-free immunosuppressive regimen. New Engl J Medicine *343*, 230 238. https://doi.org/10.1056/nejm200007273430401.

70. Kaestner, K.H., Powers, A.C., Naji, A., Consortium, H., and Atkinson, M.A. (2019). NIH Initiative to Improve Understanding of the Pancreas, Islet, and Autoimmunity in Type 1 Diabetes: The Human Pancreas Analysis Program (HPAP). Diabetes *68*, 1394–1402. https://doi.org/10.2337/db19-0058.

71. Shapira, S.N., Naji, A., Atkinson, M.A., Powers, A.C., and Kaestner, K.H. (2022). Understanding islet dysfunction in type 2 diabetes through multidimensional pancreatic phenotyping: The Human Pancreas Analysis Program. Cell Metab. *34*, 1906–1913. https://doi.org/10.1016/j.cmet.2022.09.013.

Figure 1

A

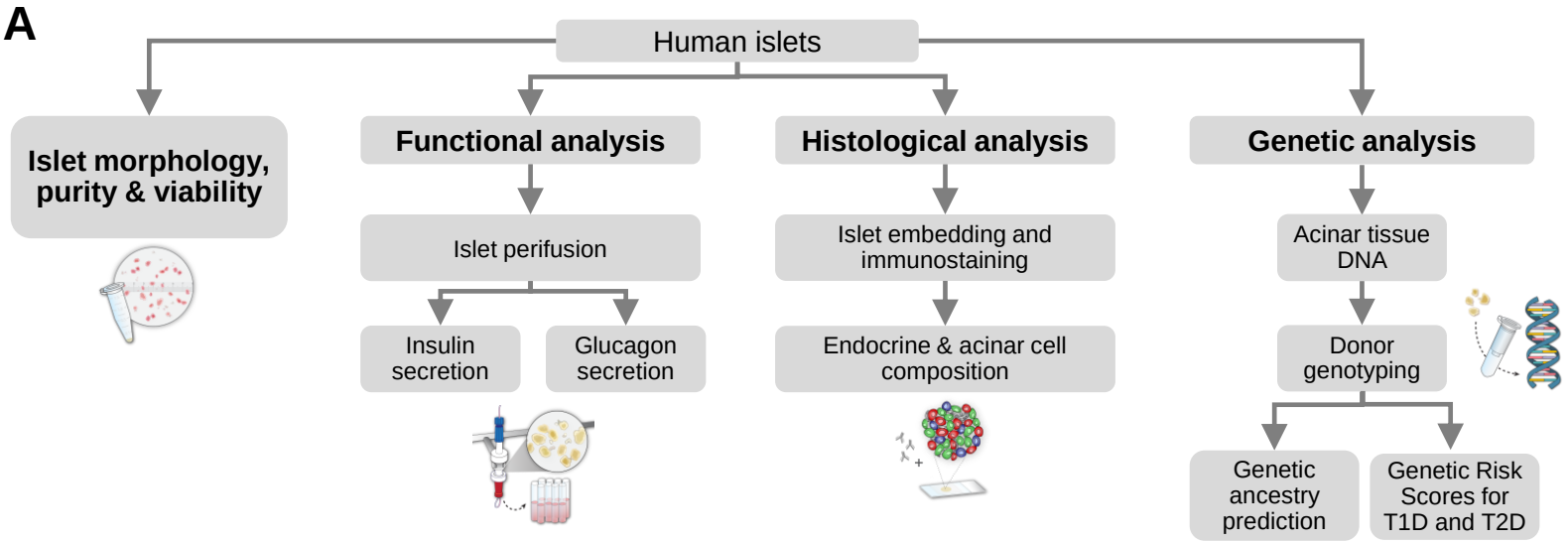

B

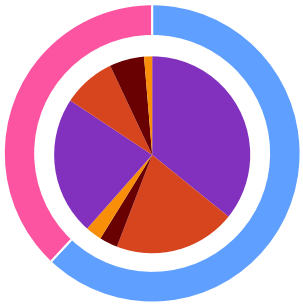

N = 299

Sex: Female Male

Reported race or ethnicity:
- Asian
- Black or African American
- Hispanic or Latino/a
- White

Reported race or ethnicity	Female (38%)				Male (62%)			
	% (N)	Age (yr)	BMI (kg/m^2)	HbA1C (%)	% (N)	Age (yr)	BMI (kg/m^2)	HbA1C (%)
Asian	3% (4)	49 ± 6 (43 – 57)	28.5 ± 4.8 (23.2 – 32.9)	5.5 ± 0.17 (5.3 – 5.6)	4% (8)	49 ± 13 (31 – 66)	26.5 ± 3.0 (21.6 – 29.9)	5.4 ± 0.33 (5.0 – 5.9)
Black or African American	15%** (17)	48 ± 14 (20 – 65)	30.6 ± 7.2 (18.2 – 47.6)	5.5 ± 0.42 (4.5 – 6.2)	5% (9)	47 ± 9 (37 – 62)	30.7 ± 6.9 (25.0 – 46.8)	5.5 ± 0.36 (5.0 – 6.1)
Hispanic or Latino/a	23% (26)	44 ± 12 (24 – 64)	30.0 ± 4.4 (22.9 – 38.7)	5.4 ± 0.42 (4.3 – 6.0)	33% (60)	40 ± 13 (15 – 62)	29.3 ± 4.7 (18.2 – 39.5)	5.5 ± 0.34 (4.5 – 6.1)
White	59% (68)	46 ± 10 (21 – 65)	28.9 ± 6.2 (17.6 – 45.5)	5.3 ± 0.43 (4.4 – 6.4)	58% (107)	45 ± 12 (17 – 68)	28.6 ± 4.8 (13.7 –40.7)	5.3 ± 0.39 (4.0 – 6.3)
Combined	38% (115)	46 ± 11 (20 – 65)	29.4 ± 5.9 (17.6 – 47.6)	5.3 ± 0.42 (4.3 – 6.4)	62% (184)	43 ± 13 (15 – 68)	28.8 ± 4.9 (13.7 – 46.8)	5.4 ± 0.37 (4.0 – 6.3)

Values reported as mean ± SD (range)

C

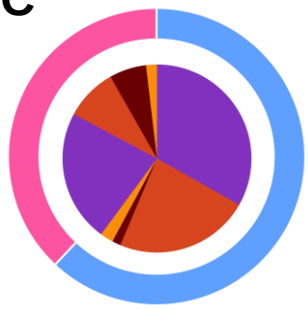

N = 268

Sex: Female Male

Primary predicted ancestry:
- East Asian
- African
- Admixed American
- European

Primary predicted ancestry	Female (40%)				Male (60%)			
	% (N)	Age (yr)	BMI (kg/m^2)	HbA1C (%)	% (N)	Age (yr)	BMI (kg/m^2)	HbA1C (%)
East Asian	5% (5)	48.2 ± 4 (43 – 57)	29.0 ± 4.3 (23.2 – 32.9)	5.4 ± 0.2 (5.2 – 5.6)	4% (6)	51.3 ± 15 (31 – 66)	25.9 ± 3.3 (21.6 – 29.9)	5.5 ± 0.3 (5.1 – 5.9)
African	16%*** (17)	48.5 ± 14 (20 – 65)	30.6 ± 7.2 (18.2 – 47.6)	5.5 ± 0.4 (4.5 – 6.2)	2.5% (4)	46.5 ± 9 (37 – 58)	32.4 ± 9.8 (25 – 46.8)	5.7 ± 0.4 (5.1 – 6.1)
Admixed American	22%** (24)	44.9 ± 12 (24 – 61)	29.6 ± 4.7 (22 – 38.7)	5.4 ± 0.4 (4.3 – 5.9)	38.5% (62)	39.6 ± 13 (15 – 62)	29.4 ± 4.8 (18.2 – 40)	5.4 ± 0.3 (4.5 – 6.1)
European	57% (61)	46.4 ± 10 (21 – 65)	28.9 ± 6.4 (17.6 – 45.5)	5.3 ± 0.4 (4.4 – 6.4)	55% (89)	46.0 ± 12 (18 – 68)	28.4 ± 5.0 (13.7 – 40.7)	5.3 ± 0.4 (4.0 – 6.3)
Combined	40% (107)	46 ± 11 (20 – 65)	29.4 ± 6.1 (17.6 – 47.6)	5.4 ± 0.42 (4.3 – 6.4)	60% (161)	44 ± 13 (15 – 68)	28.8 ± 5.0 (13.7 – 46.8)	5.4 ± 0.37 (4.0 – 6.3)

Values reported as mean ± SD (range)

Figure 2

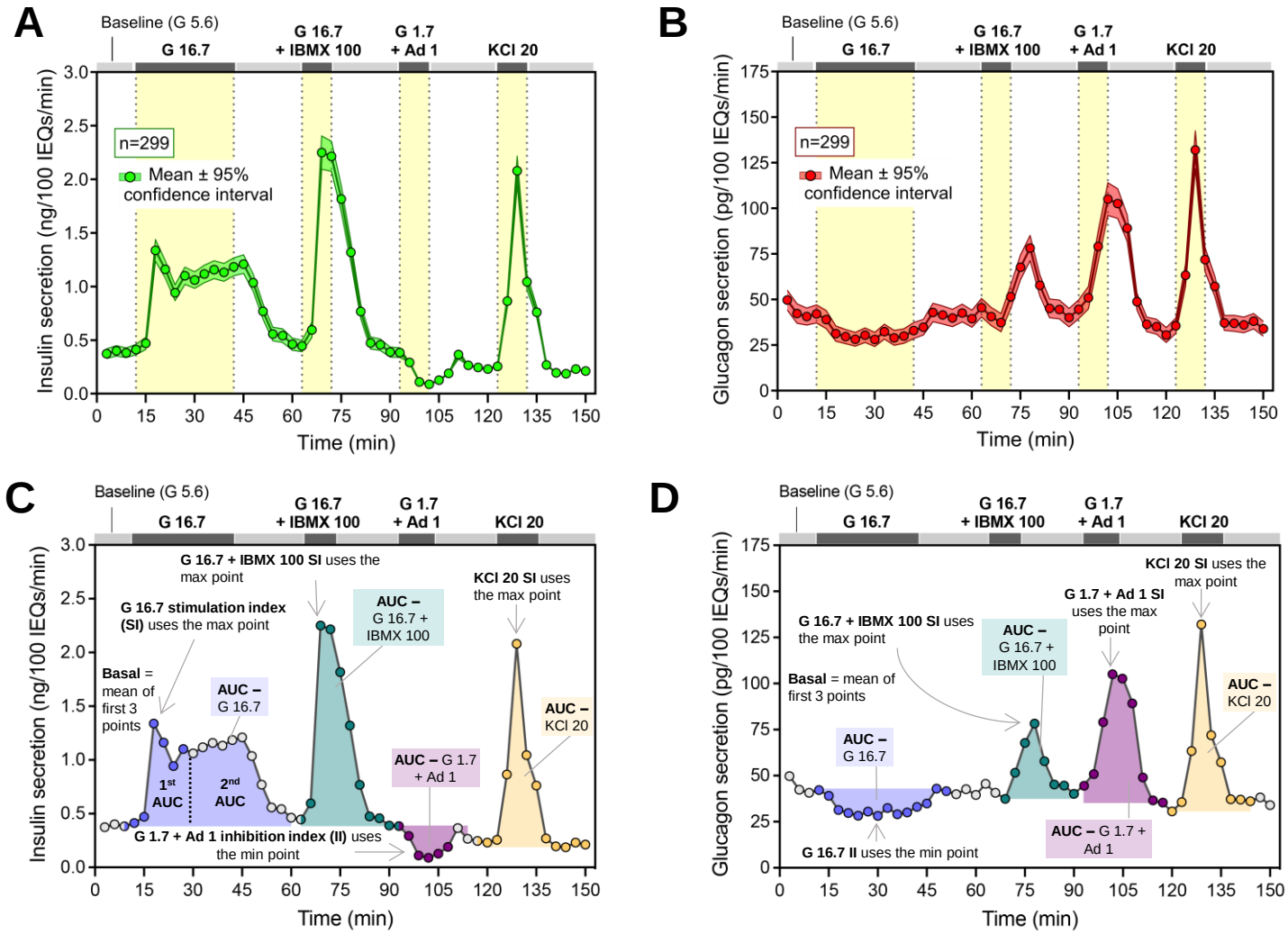

Secretagogue	Purpose	Time (start – end)	Duration (min)	Baseline	AUC (range)	SI / II (range)
Basal glucose	Baseline	0-12	12	3-9	-	-
High glucose	Glucose-stimulated insulin secretion	12-42	30	3-6 (SI) 3-12 (16.7 1st AUC) 9,60 (16.7 AUC)	3-24 (16.7 1st) 9-60 (16.7)	9-27
Basal glucose	-	42-63	21	-	-	-
High glucose + IBMX	cAMP signaling potentiation	63-72	9	60-63 (SI) 63,90 (AUC)	63-90	63-90
Basal glucose	-	72-93	21	-	-	-
Low glucose + adrenaline	Insulin inhibition	93-102	9	90-93 (II) 93,120 (AUC)	93-120	90-108
Basal glucose	-	102-123	21	-	-	-
Glucose + KCl	Membrane depolarization	123-132	9	117-120 (SI) 120,150 (AUC)	120-150	120-150
Basal glucose	-	132-150	18	-	-	-

Secretagogue	Purpose	Time (start – end)	Duration (min)	Baseline	AUC (range)	SI / II (range)
Basal glucose	Baseline	0-12	12	3-6	-	-
High glucose	Glucagon inhibition	12-42	30	3-6 (II) 3-6 (AUC)	3-63	3-42
Basal glucose	-	42-63	21	-	-	-
High glucose + IBMX	cAMP signaling potentiation	63-72	9	60-63 (SI) 69,90 (AUC)	69-90	63-90
Basal glucose	-	72-93	21	-	-	-
Low glucose + adrenaline	Glucagon secretion	93-102	9	90-93 (SI) 93,117 (AUC)	93-117	93-117
Basal glucose	-	102-123	21	-	-	-
Glucose + KCl	Membrane depolarization	123-132	9	117-120 (SI) 120,144 (AUC)	120-144	120-144
Basal glucose	-	132-150	18	-	-	-

G 16.7 2nd AUC was calculated by subtracting the G 16.7 1st AUC from the total G 16.7 AUC.

Figure 3

n = 115 female, *n* = 184 male

A

Insulin secretion traits

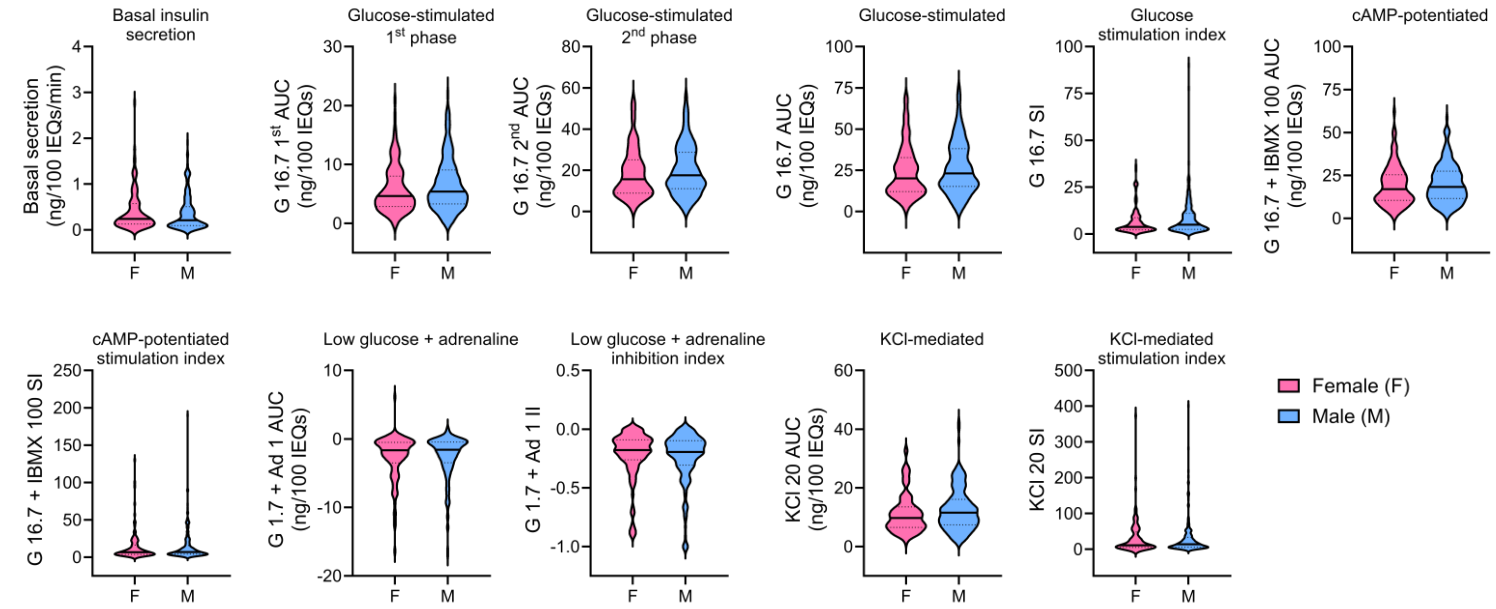

B

Glucagon secretion traits

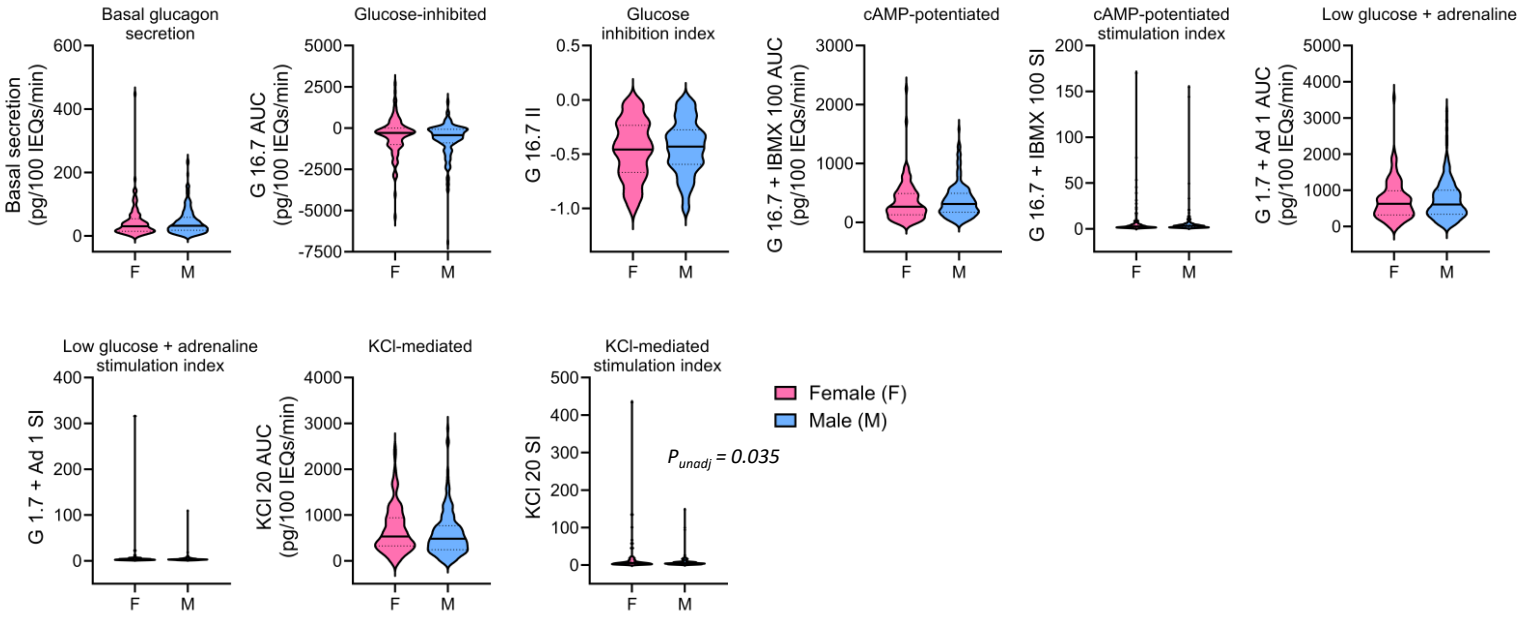

Figure 4

n = 12 Asian, *n* = 26 Black or African American, *n* = 86 Hispanic or Latino/a, *n* = 175 White

A

Insulin secretion traits

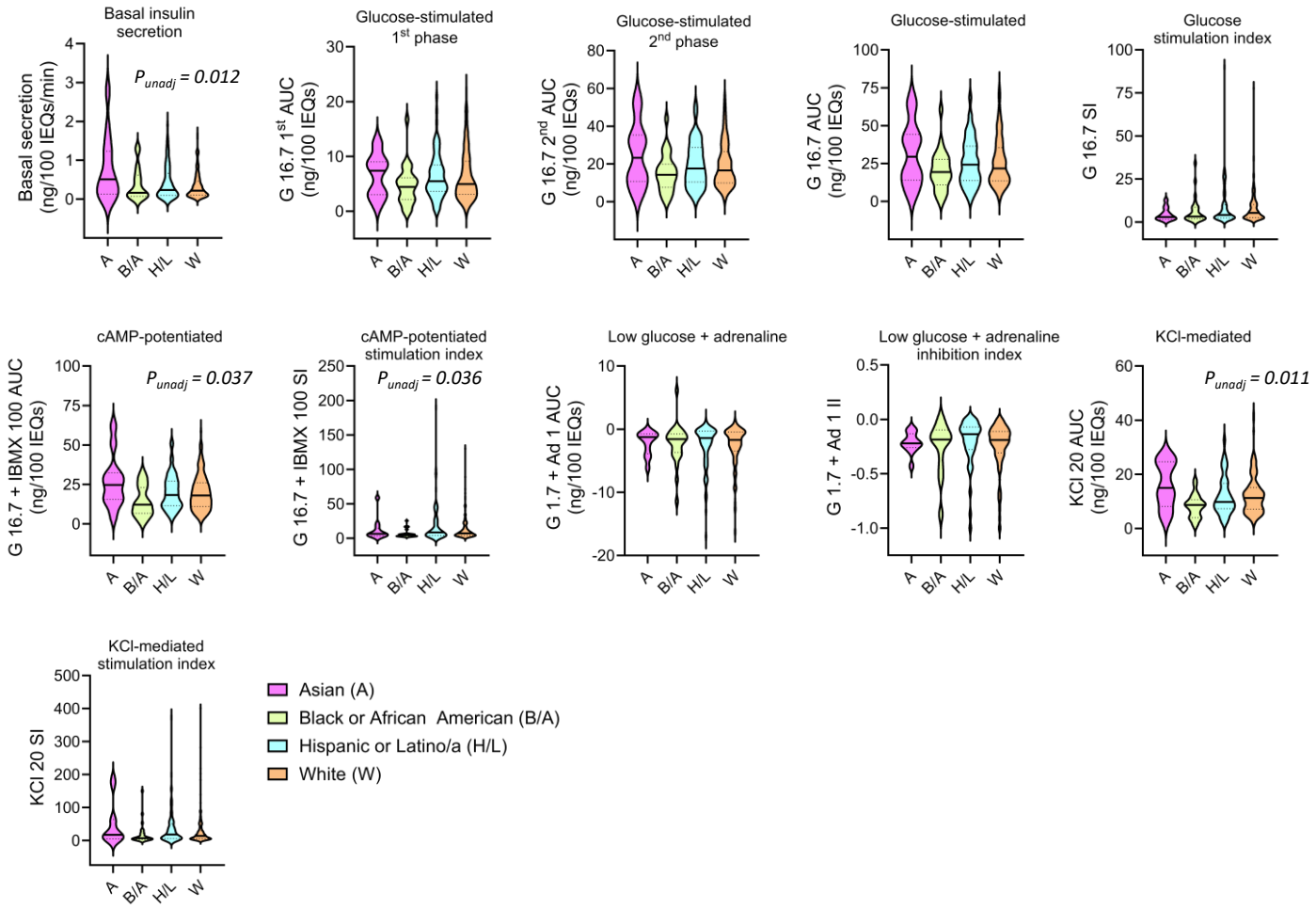

B

Glucagon secretion traits

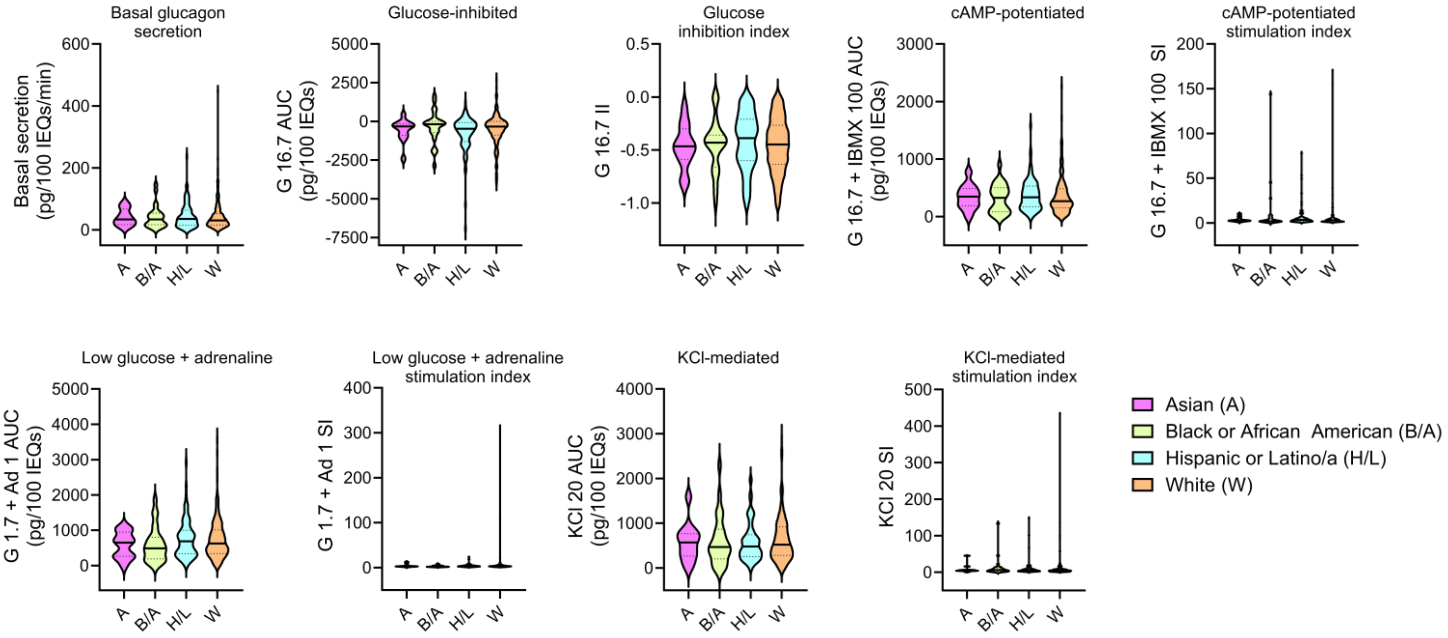

Figure 5

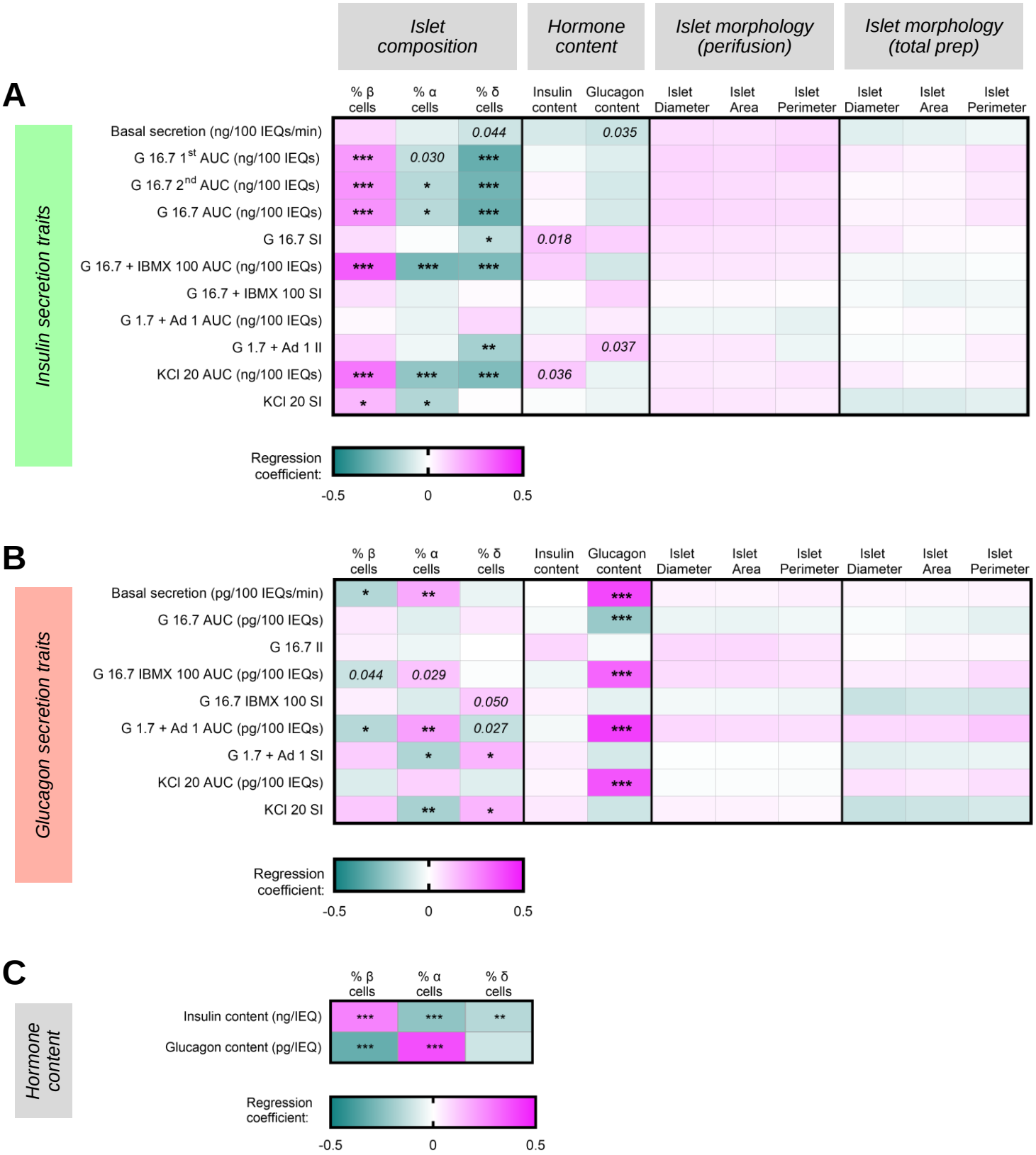
A
Islet composition
Hormone content
Islet morphology (perifusion)
Islet morphology (total prep)
% β cells
% α cells
% δ cells
Insulin content
Glucagon content
Islet Diameter
Islet Area
Islet Perimeter
Islet Diameter
Islet Area
Islet Perimeter
Insulin secretion traits
Basal secretion (ng/100 IEQs/min)
G 16.7 1st AUC (ng/100 IEQs)
G 16.7 2nd AUC (ng/100 IEQs)
G 16.7 AUC (ng/100 IEQs)
G 16.7 SI
G 16.7 + IBMX 100 AUC (ng/100 IEQs)
G 16.7 + IBMX 100 SI
G 1.7 + Ad 1 AUC (ng/100 IEQs)
G 1.7 + Ad 1 II
KCl 20 AUC (ng/100 IEQs)
KCl 20 SI
Regression coefficient:
-0.5
0
0.5
B
Glucagon secretion traits
Basal secretion (pg/100 IEQs/min)
G 16.7 AUC (pg/100 IEQs)
G 16.7 II
G 16.7 IBMX 100 AUC (pg/100 IEQs)
G 16.7 IBMX 100 SI
G 1.7 + Ad 1 AUC (pg/100 IEQs)
G 1.7 + Ad 1 SI
KCl 20 AUC (pg/100 IEQs)
KCl 20 SI
Regression coefficient:
-0.5
0
0.5
C
Hormone content
Insulin content (ng/IEQ)
Glucagon content (pg/IEQ)
Regression coefficient:
-0.5
0
0.5

Figure 6

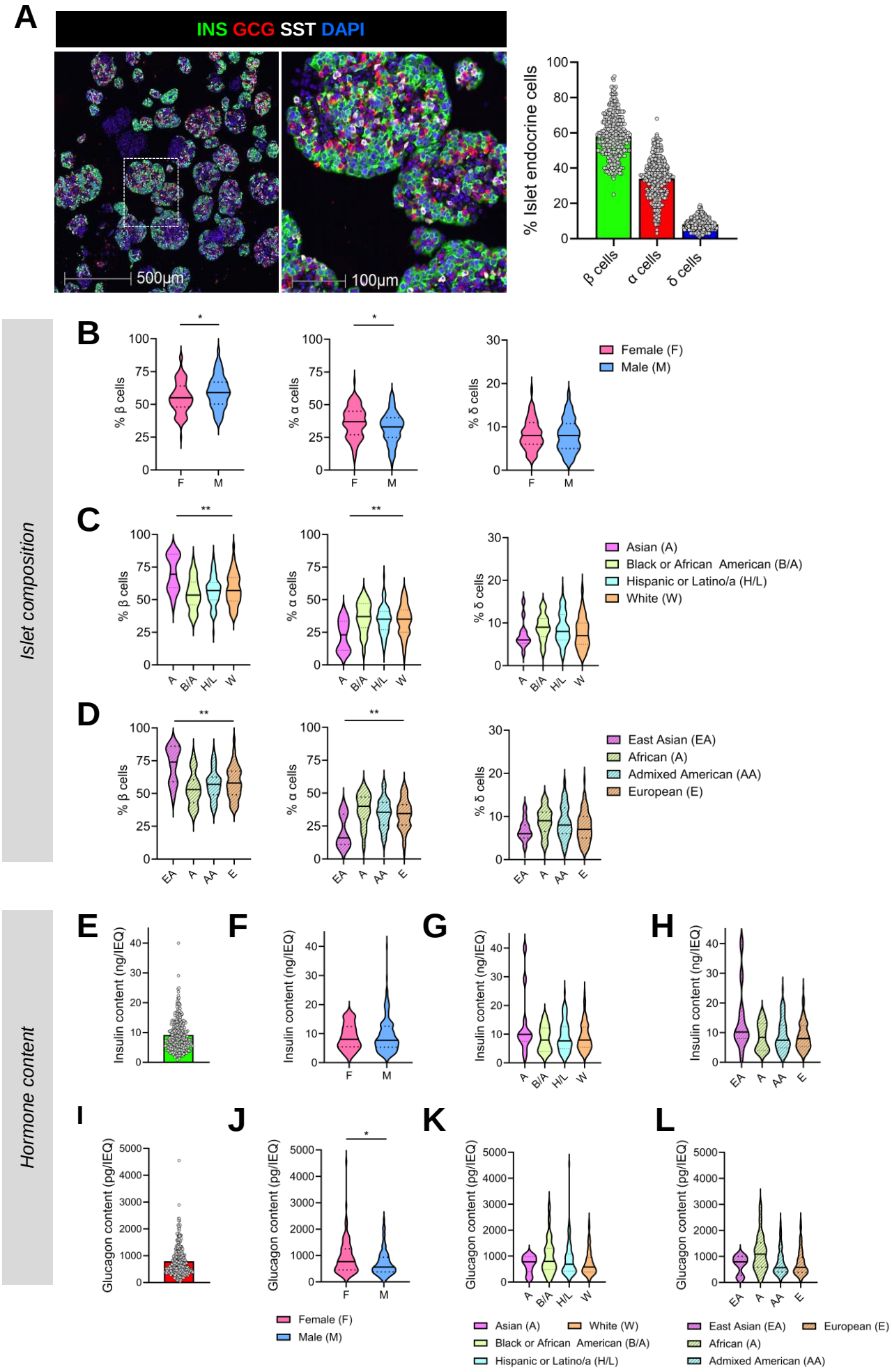
A
INS GCG SST DAPI
500µm
100µm
% Islet endocrine cells
β cells
α cells
δ cells
Islet composition
B
% β cells
% α cells
% δ cells
F
M
Female (F)
Male (M)
C
Asian (A)
Black or African American (B/A)
Hispanic or Latino/a (H/L)
White (W)
D
East Asian (EA)
African (A)
Admixed American (AA)
European (E)
Hormone content
E
F
G
H
Insulin content (ng/IEQ)
I
J
K
L
Glucagon content (pg/IEQ)

Figure 7

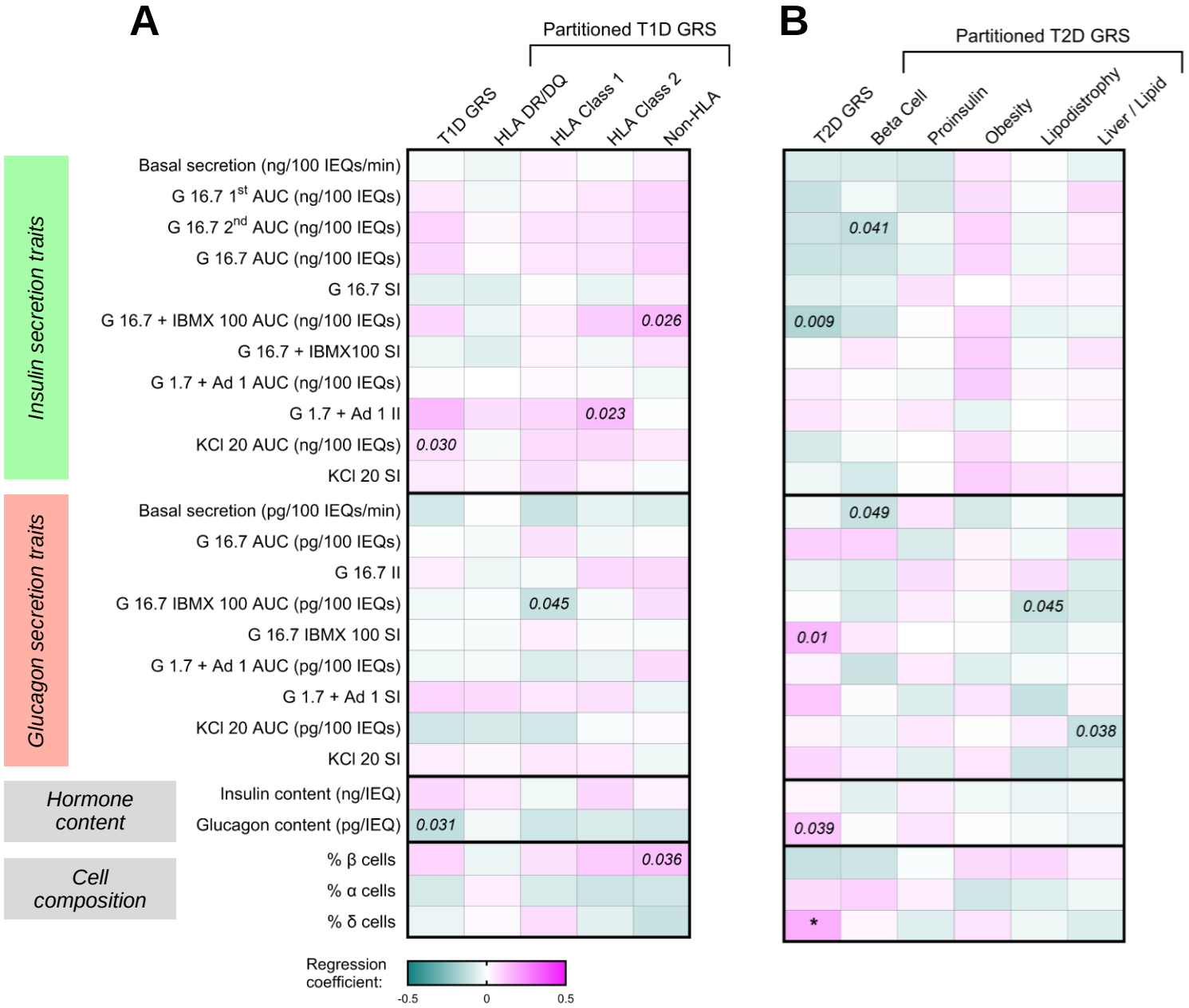
A
Partitioned T1D GRS
T1D GRS
HLA DR/DQ
HLA Class 1
HLA Class 2
Non-HLA
Insulin secretion traits
Basal secretion (ng/100 IEQs/min)
G 16.7 1st AUC (ng/100 IEQs)
G 16.7 2nd AUC (ng/100 IEQs)
G 16.7 AUC (ng/100 IEQs)
G 16.7 SI
G 16.7 + IBMX 100 AUC (ng/100 IEQs)
G 16.7 + IBMX100 SI
G 1.7 + Ad 1 AUC (ng/100 IEQs)
G 1.7 + Ad 1 II
KCl 20 AUC (ng/100 IEQs)
KCl 20 SI
Glucagon secretion traits
Basal secretion (pg/100 IEQs/min)
G 16.7 AUC (pg/100 IEQs)
G 16.7 II
G 16.7 IBMX 100 AUC (pg/100 IEQs)
G 16.7 IBMX 100 SI
G 1.7 + Ad 1 AUC (pg/100 IEQs)
G 1.7 + Ad 1 SI
KCl 20 AUC (pg/100 IEQs)
KCl 20 SI
Hormone content
Insulin content (ng/IEQ)
Glucagon content (pg/IEQ)
Cell composition
% β cells
% α cells
% δ cells
0.026
0.023
0.030
0.045
0.031
0.036
B
Partitioned T2D GRS
T2D GRS
Beta Cell
Proinsulin
Obesity
Lipodistrophy
Liver / Lipid
0.041
0.009
0.049
0.045
0.01
0.038
0.039
*
Regression coefficient:
-0.5
0
0.5